

A multiscale signalling network map of innate immune response in cancer reveals signatures of cell heterogeneity and functional polarization

Maria Kondratova^{1,3}, Urszula Czerwinska^{1,3,5}, Nicolas Sompairac¹, Sebastian D Amigorena², Vassili Soumelis², Emmanuel Barillot¹, Andrei Zinovyev^{1,4} and Inna Kuperstein^{1,4*}

¹Institut Curie, PSL Research University, Mines Paris Tech, Inserm, U900, F-75005, Paris, France

²Institut Curie, PSL Research University, Inserm, U932, F-75005, Paris, France

³Equal contribution

⁴Senior authors

⁵Université Paris Descartes, Centre de Recherches Interdisciplinaires, Paris, France

*Correspondence: inna.kuperstein@curie.fr

SUMMARY

Lack of integrated resources depicting the complexity of innate immune response in cancer represents a bottleneck in the integration and interpretation of high-throughput data. To address this challenge, we performed systematic manual literature mining of molecular mechanisms governing innate immune response in cancer and represented it as an integrated signalling network map, where the knowledge was organised in a hierarchical and multiscale manner.

First, the individual cell-type specific signalling maps were constructed for macrophages, dendritic cells, myeloid-derived suppressor cells and natural killers. The cell type-specific maps were integrated into a comprehensive meta-map of innate immune response in cancer, depicting functional modules collectively contributing to anti- and pro-tumor signalling. Intuitive map exploration is enabled through our Google Maps-based NaviCell web platform. The meta map contains 1466 nodes among which there are 582 proteins, 1084 biochemical reactions and it is supported by information from 837 cell type specific and cancer-relates articles.

The cell type-specific signalling maps together with the meta-map of innate immune response in cancer form an open web-based platform. This unique resource allows deciphering the heterogeneity of cell populations in the tumor microenvironment (TME). All the developed maps are available online (<http://navicell.curie.fr/pages/maps.html>). It can be applied for innate immune status inference and making prognosis from based on tumor molecular profiling

The cell type-specific maps and the meta-map were used to interpret single cell RNA-Seq data from macrophages and natural killer (NK) cells in metastatic melanoma. The analysis demonstrated existence of sub-populations within each cell type that possess anti- and pro-tumor polarization status. Macrophage population consists of two types of cells, one is characterized by anti-tumor activity, whereas the second one is oriented towards pro-tumor activity. Activated subset of NK cells were characterized by induction of LFA1, CR3 and FcGR2 pathways involved in triggering tumor-killing signaling, indicating anti-tumor polarization status of NK in the studied sub-sets of cells.

Key words

Tumor immunology, tumor microenvironment, innate immunity signalling, cancer systems biology, comprehensive signalling network map, semantic zooming, single cell data analysis, bioinformatics, molecular pathways and networks, intercellular communication, cell reprogramming, polarization, heterogeneity

INTRODUCTION

Tumors are engulfed in a complex microenvironment (TME) that critically impacts disease progression and response to therapy. TME includes immune and non-immune interconnected components exchanging multiple signals and influenced by molecules secreted by cancer cells. The behavior of the tumor and its TME as a whole critically depends on the organization of these different players and their ability to regulate each other in a dynamic manner (Becht et al., 2016). The innate immune part of TME plays important, but sometimes opposite roles in tumor evolution. Innate immune cells can contribute to the elimination of tumor, e.g. through phagocytosis and T cell priming and by induction of adaptive immune response. However, they can also favor tumor escape from immunological control by a production of immunosuppressive molecules such as TGFB, IL10 and growth factors (Cali et al., 2017). An additional level of complexity in the TME is that various stimuli can lead to a range of innate immune cells phenotypes. This results in very heterogeneous sub-populations within each innate immune cell type coexisting in TME (Laoui et al., 2011), (Van Overmeire et al., 2014)(Chávez-Galán et al., 2015).

Depending on the set of stimuli from TME and tumor, immune cells are able to change their phenotype or polarization status from anti-tumor or pro-tumor (Vesely et al., 2011). Such functional dichotomy was first evidenced for one of the components of innate immunity in TME, the tumor-associated macrophages (TAM) and led to a description of M1 and M2 polarized TAM classes (Goswami et al., 2017). The same tendency was later documented for other components of innate immunity as Neutrophils (Fridlender and Albelda, 2012), Dendritic Cells (Gordon et al., 2014) and Natural Killers (Cooper et al., 2001). Therefore, the term ‘polarization’ can be applied for the innate immunity system in TME in general (Mittal et al., 2014) that represents the major interest of current works. The balance between anti-tumor and pro-tumor activity of innate immune cells has an impact on tumor growth, patient response to therapy and survival (Marvel and Gabrilovich, 2015).

Correct evaluation of the polarization status within the subtle innate immune cell sub-populations in TME is essential for immunotherapy improvement. Immune checkpoint targeting significantly changed the place of immunotherapy in cancer care. The most known immune therapeutic targets are PD-1/PD-L1 and CTLA-4, which inhibit adaptive (T cell) responses in tumors (Topalian et al., 2015). Currently, the majority of efforts are still invested into an identification of additional immune targets in the adaptive immune system (Torphy et al., 2017). However, the primary activation of adaptive immune response requires innate immune players, the antigen presenting cells (APC) such as dendritic cells (Vo et al., 2017) or macrophages (Mantovani et al., 2017)(Bonelli et al., 2017). Therefore, an efficiency of immune checkpoint therapy is directly dependent on proper innate immune activation (Moynihan and Irvine, 2017). In addition, there are studies showing that innate immunity can restrict tumor growth even when the adaptive immune system is

inactivated (O’Sullivan et al., 2012). This indicates that detailed study of potential innate immune-related targets should be performed to identify new types of immunotherapy (Tokunaga et al., 2018) that could function in synergy with the current T cell-targeted therapies or act independently (Bellora et al., 2017)(Gebremeskel et al., 2017).

There is a massive information in the literature about molecular mechanisms implicated in innate immune cells polarization in TME. However, most of the studies are focused on individual molecular components and pathways. They do not integrate the complexity of multiple crosstalk between innate immune cells and tumor. Similarly, there exists a number of immune-related gene signatures in different cancer types and stages, serving as immune status biomarkers and prognostic factors (Ascierto et al., 2011; Clark, 2017; Garg et al., 2017). However, the signatures do not explain the molecular mechanisms of polarization of innate immune cells in TME. To create a holistic picture of diversity and integrity of innate immune system in TME, the knowledge about molecular circuits should be gathered together and systematically represented (Kreuzinger et al., 2017).

To address these challenges, a systems biology approach is needed (Bhinder and Elemento, 2017). Formalization of biological knowledge in a form of comprehensive signalling maps, both at the intra- and intercellular levels helps to integrate information from multiple research papers (Dorel et al., 2015). Despite the fact that there are numerous public databases containing signalling pathways related to innate-immune response as KEGG (Kanehisa et al., 2012) and REACTOME (Croft et al., 2014), the signalling is represented there in patched manner lacking cross-regulatory links between pathways and integrated presentation of multi-cellular system of innate immunity. In addition, there are resources dedicated to different types of innate immune cells such as macrophages (Raza et al., 2008) or dendritic cells (Cavalieri et al., 2010). Finally, there are resources depicting the innate immune system in general as Innate DB (Breuer et al., 2013) and ImmuNet (Gorenshteyn et al., 2015), Virtually Immune (O’Hara et al., 2016). However, these repositories are rather pathogen response-oriented than cancer-specific and often represent a catalogue of disconnected pathways. Therefore, there is a need to create an integrated resource on molecular mechanisms of innate immune response in cancer. To fill the gap, we constructed a system of cell type-specific maps and an integrated meta-map of innate immune signalling in cancer based on the information retrieved from the literature (Figure 1). These maps together represent an open source analytic platform for data interpretation and modelling of TME in cancer and other human diseases.

RESULTS

Principles of innate immunity map construction and annotation

To cope with a massive body of literature on innate immune response in cancer we followed a systematic procedure of literature selection, knowledge organisation and integration of information in a visual and understandable manner (Figure 1). The network map is constructed as a two-dimensional map to facilitate a graphical representation of molecular mechanisms that drive biological processes. The map normally possesses a particular layout that reflects the accepted vision of spatial organisation and propagation of biological processes. Molecular mechanisms regulating six innate immune cell types found in the TME are gathered and depicted in the form of network maps. The information

about molecular mechanisms was manually retrieved by the map managers from the scientific literature along with the information presented in general pathway databases or in the immune system-specialized resources. The information was classified by specificity to the innate immune cell-types in cancer and organized into three cell-types specific signalling network maps, namely map of macrophages and myeloid-derived suppressor cells, dendritic cells and natural killer cells (Figure 2). These maps, enriched by the information on additional cell types as neutrophils and mast cells, were integrated into the meta-map of innate immune response in cancer (Figure 3).

The molecular mechanisms are depicted on the maps in the form of biochemical reaction network using well-established methodology (Kondratova et al., 2016)(Kuperstein et al., 2015). The maps are constructed using Systems Biology Graphical Notation language (SBGN) (Le Novère et al., 2009) as drawn in CellDesigner tool (Kitano et al., 2005) that ensures compatibility of the maps with various tools for network analysis, data integration and network modelling (Figure 3B). Each molecular player and reaction in the maps is annotated in the NaviCell format. The NaviCell annotations include PubMed references, cross-references with other molecular biology databases and notes of the map manager. In addition, each molecular player and reaction is assigned with the confidence score and tags that indicate involvement in different biological processes on the map (Supplemental Figure 1).

The principles and procedure of map construction, including the graphical standard, data model, rules of literature curation, data input from other databases and the detailed tagging system description are provided in the Methods section. In the future, the cell type-specific and the meta-map of innate immune response will become a part of the Atlas of Cancer Signalling Network resource (ACSN, <http://acsn.curie.fr>) and a tool for interactive web-based data visualization (Kuperstein et al., 2015).

Content and structure of the maps: inter- and intra-cellular signalling

Cell type-specific maps

The most studied and comprehensively described cell types in TME as macrophages and MDSC, dendritic cells and natural killers are represented in a form of individual cell type-specific maps. The correspondence of the mechanisms to anti- or pro-tumor activity for each cell type is indicated (Figure 2 and Supplemental Table 1). However, neutrophils and mast cells are less studied and molecular mechanisms implicated in the regulation of these cell types in TME is limited. The available knowledge on the neutrophils and mast cells in TME is included only into the meta-map of innate immune response in cancer (Figure 3 and Table 1).

Macrophages and myeloid-derived suppressor cells in cancer

Macrophages are the major immune component of leucocyte infiltration in the tumor. The main markers of macrophage are CD11b+, CD68+, LGALS+ and CD163. The anti-tumor polarization of macrophages is related to their ability to recognize and to reject tumor cells by phagocytosis, represent tumor antigens on the cell surface and induce a T-cell response. Macrophages produce cytotoxic agents such as Reactive Oxygen Species and Nitrite Oxide, secrete chemokines as CXCL-8, CCL2, CCL3, etc. and attract immune cells into the TME. It addition, they express inflammatory cytokines as TNF, IL12, IL1, etc. facilitating local immunity activation. Tumor-associated macrophages (TAMs) can also act as pro-tumor agents, expressing tumor stimulating growth factors as PDGF, EGF, VEGF, FGF, producing immunosuppressive molecules as IL10 and TGFB, that induce angiogenesis and matrix remodelling in TME

and consequently facilitate metastatic process (Biswas and Mantovani, 2010; Murray and Wynn, 2011)

Myeloid-derived suppressor cells (MDSC) represent a heterogeneous population of myeloid cells. In general, the role of MDSC in TME is similar to TAMs. Their main surface markers are CD33+, CD15+ (granulocytic), CD14+ (monocytic), CD34+ and CD11b+. MDSC suppress T-cell response and Natural killers' activity via TGFB signalling and arginine depletion from TME. In addition, MDSCs induce EMT and angiogenesis and participates in matrix remodelling via VEGF and MMPs secretion. MDSC mostly show a pro-tumor activity, therefore their presence in the tumor is correlated with a poor clinical prognosis (Gabrilovich and Nagaraj, 2009; Ostrand-Rosenberg and Sinha, 2009). The MDSC signalling is included into the Macrophage cell type-specific map.

The macrophage and MDSC cell type-specific map contains 588 objects and 7 modules represented both pro-tumor and anti-tumor polarization of myeloid cells. Pro-tumor zone includes module "Immunosuppressive cytokine pathways". Anti-tumor zone contains modules: "Immunostimulatory cytokine pathways", "Immunostimulatory cytokine expression", "Antigen presentation", "No and ROS production". Modules "Core signalling pathways" and "Recruitment of immune cells" form a natural border between pro- and anti-tumor zones (Figure 2A and Supplemental Table 1). and the map is available at http://navicell.curie.fr/pages/maps_macrophage.html.

Dendritic cells in cancer

Dendritic cells (DC) are innate immune cells that can have both myeloid and lymphoid origin. The main marker for mature dendritic cells is CD83+. Immature dendritic cells express among others HLA-DR, CD80, CD86, CD1a, CD40, CD14, CD11c, CD209, ILT3. As with macrophages, dendritic cells possess phagocytic abilities and can produce inflammatory cytokines as IFNs, IL12, etc. The major role of dendritic cells in anti-tumor response is antigen presentation and T-cell activation. (Palucka and Banchereau, 2012) . The DC map contains 491 objects and 8 modules (Figure 2B and Supplemental Table 1) Pro-tumor zone of the map contains modules "Immunosuppressive cytokine pathways", "Immunosuppressive checkpoints". Anti-tumor zone contains modules: "Immunostimulatory cytokine pathways", "Antigen presentation", "Tumor recognition and tumor killing", "DC markers", modules "Core signalling pathways" and "Recruitment of immune cells" form a border between pro- and anti-tumor zones.

The map is available at http://navicell.curie.fr/pages/maps_dendritic.html.

Natural killers cells in cancer

Natural killers (NK) are big granular lymphocytes which can be cytotoxic to tumor cells. The markers of this cell type are specific NK-receptors as NKp30, NKp46, NKG2D, etc. The main role of NK cells in innate immunity is an elimination of cells lacking MHC1 molecules that therefore cannot be recognized by T-cells. NK are stimulated by the target cells expressing NK receptors activating ligands such as MICA, MICB, etc. The activity of NK cells is modulated by inflammatory cytokines as IL15, IL12, produced by macrophages and dendritic cells. NK cells secrete granules contains lytic enzymes (granzymes, perforin, granzulin, etc) and express apoptosis inducers TRAIL and FASL. Presence of active NK cells in cancer is correlated with good prognosis. To escape NK control, tumor cells express immunosuppressive ligands as MIF, IL10, TGFB, and downregulation of NK ligands expression that collectively inhibit cytotoxic activity of NK cells (Vivier et al., 2012). A pro-tumor polarization of NK cells is not described in the literature. However, suppressed NK cells are incapable to reject tumor cells and therefore indirectly

promote cancer progression. The NK map contains 567 objects and 6 modules (Figure 2C and Supplemental Table 1). Pro-tumor zone of the map contains modules “Immunosuppressive cytokine pathways”, “NK inhibiting receptors”. Anti-tumor zone contains modules: “Immunostimulatory cytokine pathways”, “NK activating receptors”, “Lytic granules exocytosis”, module “Core signalling pathways” forms a border between pro- and anti-tumor zones.

It is available at http://navicell.curie.fr/pages/maps_natkiller.html.

Neutrophil cells in cancer

Neutrophils form a subtype of granulocytic leukocytes. The main markers of this cell type are (FUT4, CD16, ITGA4(-)). The role of neutrophils in the tumor microenvironment is not well documented, but it is known that they can produce ROS, inflammatory cytokines and demonstrate tumoricidal activity. Though in other conditions neutrophils act as pro-tumor agents via stimulation of matrix remodelling, angiogenesis and metastasis, therefore these cells have both pro and-antitumor polarization potential (Fridlender and Albelda, 2012; Fridlender et al., 2009) . The signalling on neutrophils is included into the innate immune meta-map (Figure 3 and Table 1).

Mast cells in cancer

Mast cells resemble blood basophils and contain granules rich in histamine and heparin (markers: FCER2, KIT, ENPP3, FCER1A). Experimental data about the influence of mast cell on tumor microenvironment is contradictory. It is known that mast cells can produce inflammatory cytokines IL1, IL6, TNF, INF α and secrete Chondroitin sulphate which acts as a decoy for tumor cells and blocks the metastatic process. However, mast cells also secrete molecules stimulating tumor growth, angiogenesis and local immunosuppression (Tryptase, Heparin, IL8, VEGF, NGF, PDGF, SCF, Histamine) (Marichal et al., 2013; Theoharides and Conti, 2004) . Probably the polarization of mast cells in TME is context-dependent. The signalling on mast cells is included into the innate immune meta-map (Figure 3 and Table 1).

Integrated hierarchical modular meta-map of innate immune response in cancer

The aforementioned cell type-specific maps gathered together and enriched by additional information, gave rise to the global, seamless meta-map of innate immunity in cancer. The layout design of the meta-map reflects the current understanding of signalling propagation in cells. To cope with the complexity of the signalling network and to make it understandable and navigable, the meta-map has a hierarchical structure (Figure 1 and Figure 3). The meta-map possesses two major structuring dimensions: the internal organisation of the map (layers, zones, modules, pathways) and external organisation represented by zoom levels (see the explanation below).

The internal organisation of the meta-map is provided in a form of *three layers*: Inducers, Core signalling and Effectors (Figure 3B and Table 1). The top part of the meta-map depicts inducer molecules frequently present in TME (layer ‘Inducers’). The inducers interact through specific receptors and adaptor proteins that propagate the signal via limited number of transmitters, also called hub molecules as NF- κ B, PLCG, PI3K etc. These molecules are located in the middle parts of the meta-map in the layer Core signalling. The signalling is further propagated to the layer Effectors which are located in the lower part of the meta-map. The latest entities actually execute the biological activity and therefore define the outcome phenotype, namely, the positive or negative influence of the innate immunity system on

the tumor growth and invasion (Figure 3B and Table 1).

Further, the whole meta-map is divided into multiple *signalling pathways*, running through the aforementioned layers. (Figure 3B) We define a signalling pathway as a natural sequence of molecular interactions which transform extracellular signal into intracellular activity. The pathways include all macromolecules as proteins, RNA, genes, etc. participating or influenced by a certain ligand or receptor and leading to a particular cell outcome indicated by phenotypes such as Tumor Killing, Tumor Growth, etc. Usually, pathways are named after the first molecule in the sequence, which is a ligand (e.g. TNF pathway, IL10 pathway), but in the cases when several ligands act through the same receptor, a signalling pathway receives the name of the corresponding receptor-ligand complex (e.g. TLR2/4 pathway). The meta-map is composed of 98 signalling pathways, 30 of which contain more than 10 molecules in the sequence (Supplemental Table 2). It is worth highlighting that there are many cross-talks between different signalling pathways (Figure 3B). The signalling pathways on the meta-map are useful for retrieving the back-bone structure of the network and map reduction, especially relevant for structural analysis and modelling studies.

The signalling pathways of the meta-map form together 25 *functional modules* representing relatively independent fragments of global network responsible for execution of certain molecular functions, e.g. Antigen presentation, Exocytosis, Phagocytosis, Checkpoints, etc. The functional modules are assembled into the structures of higher level, namely 9 *biological processes (meta-modules)*, reflecting the major biological activities of innate immune system with respect to a tumor, i.e. Tumor recognition, Tumor growth, Timor killing, Immune stimulation, Immune suppression, etc. At the highest level, all biological processes are grouped into two *zones* representing the concept of innate immune system polarization into anti- or pro-tumor mode. The anti-tumor zone contains ‘Tumor recognition’, ‘Immune activation’, ‘Tumor killing’ processes, whereas the pro-tumor zone is composed of ‘Inhibition of tumor recognition’, ‘Immune suppression’ and ‘Tumor growth’ processes (Figures 1, 3A and Table 1). The list of molecules per modules and biological processes (meta-modules) is available in the Supplemental Table 3. All these levels of the map are interconnected and cross-talk to each other. The cross-talks between key biological processes is represented as an interaction network (Figure 3C) We can see a number of interactions between different parts of the map here, of different nature (activation, inhibition, molecular flow) and different scale. We can see that “Core signalling” (central point of network) play a role of the “hub” for most signalling pathways and that there are a lot of positive and negative cross-talks between immune stimulation and immune suppression in innate immunity.

The meta-map contains 1466 nodes among which there are 582 proteins, 1084 biochemical reactions and it is supported by information from 820 cell-type specific and cancer-relates articles (Table 1). The meta-map and cell specific maps are available at http://navicell.curie.fr/pages/maps_innateimmune.html.

The external organisation of the meta-map is reflected in *hierarchical structure of zoom levels*, similar to geographical maps, where on each zoom level only limited information is displayed. The meta-map contains the top zoom level, the least detailed level that schematically represent borders of Biological Processes, providing the global view on the map organisation. The contours of the meta-modules and modules are highlighted by the colourful background (Figure 3A). The next zoom level allows to appreciate the functional modules structure and the last, most detailed one provides the view on signalling pathways and detailed biochemical reactions that compose these pathways (Figure 3 B). This hierarchical structure of the map facilitates Google Maps-like navigation of the map as explained in the next section.

Access, navigation and maintenance of the innate immune response maps

The cell type-specific and the integrated meta-map are open source and can be browsed online. The user-friendly interface of the maps provides a possibility to explore the individual cell type-specific maps or to access the integrated meta-map of innate immunity in cancer. The visualization and navigation of maps are supported by the NaviCell web-based environment empowered by Google Maps engine (Kuperstein et al., 2013). The navigation features such as search, scrolling, zooming, markers, callout windows and zoom bar are adopted from the Google Maps interface. All map components are clickable, making the map interactive. The extended annotations of map components contain rich tagging system, converted to links. This allows tracing the involvement of molecules into different map sub-structures as pathways, modules, and biological processes. In addition, cell type-specific tags make clear correspondence between the cell type-specific maps and the integrated meta-map of innate immune response, allowing shuttling between the maps (Supplemental Figure 3).

The semantic zooming feature of NaviCell (Kuperstein et al., 2013) simplifies navigation through large maps of molecular interactions, showing readable amount of details at each zoom level. Gradual exclusion of details allows exploration of map content from the detailed towards the top-level view. The hierarchical structure of the innate immune response meta-map as described above, allowed to generate several zoom levels (Figure 3 A and B).

Comparison of meta-map of innate immune response in cancer with existing pathway databases

The content of the meta-map was compared with the relevant sub-set of pathways related to the innate immune system from existing molecular interaction databases. The InnateDB database contains a detailed description of the innate-immune signalling, even though more general databases as KEGG and REACTOME also include immune pathways. Pathways related to the human innate immune system were selected from the InnateDB resource, excepting ‘Complement Cascade (Human)’, ‘NOD-like Receptor Signalling Pathway’, ‘Regulation of autophagy (Human)’, ‘RIG-I-like receptor signalling pathway (Human)’. The excluded pathways represent virus and bacterial infection-specific pathways that do not correspond to TME signalling. The KEGG innate immune-related pathways were retrieved from the list “5.1 Immune system”. The pathways obtained from REACTOME cover ‘Class I MHC mediated antigen processing & presentation’ and ‘MHC class II antigen presentation’ from Adaptive Immune branch, and all pathways from Innate Immune branch (the list of selected pathways is available in the Supplemental Table 4). All together 666 gene names from Innate DB, 563 gene names from KEGG and 2156 gene names from REACTOME were selected and compared with the innate immune response meta-map that contains 683 gene names.

The selected InnateDB pathways altogether contain nearly the same number of objects as the innate immune response meta-map. The content of selected KEGG or REACTOME pathways is richer than in the innate immune response meta-map, due to the fact that KEGG and REACTOME are generic databases, describing all innate immune-related interactions, whereas the meta-maps is rather oriented to cancer signalling. The overlap between the meta-map and the three selected databases represents 61 % for InnateDB, 58% for KEGG and 30% for REACTOME. It is important to note that there are 188 genes that present exclusively at the innate immune response meta-map (Supplemental Figure 3A and Supplemental Table 4). These unique genes are relatively homogeneously distributed across the meta-map, indicating that depicted processes are described in more depth on the meta-map compared to other three databases (Supplemental Figure 3 A). There are several modules that significantly enriched by unique genes on the meta-map

(Supplemental Figure 3 B). Thus, the modules ‘Tumor growth’ and ‘Immunosuppressive checkpoints’ contain signalling that very well studied in cancer cells and therefore represented in great details on the meta-map. There are additional two modules, entitled ‘MIRNA TF immunostimulatory’ and ‘MIRNA TF immunosuppressive’, that contain the latest information on involvement of miRNA in the innate immune system control in cancer and unique for the meta-map, comparing to other databases. We concluded that the content of meta-map is relatively non-redundant with the other pathway databases and there are several functional modules directly related to TME functions, that are unique to the meta-map.

We also compared the set of publications used to annotate the four pathway databases. The overlap of the literature body in the meta-map with the three databases was small: 785 papers out of 837 papers that were used to annotate the meta-map are unique (Supplemental Figure 3B). Although the median date of annotated reference in the meta-map is only one year-younger compared with InnateDB and REACTOME, there is significant number of papers dating 2010–2017 (230 Articles (27%) out of 837). The meta-map contains more papers published after 2010 than Innate DB and REACTOME (Supplemental Figure 3C), indicating that the map contains the most recent discoveries in the corresponding fields. The meta-map uses relatively similar range of journals as the other two databases, however the specific immunological journals (such as J. of Immunology, Immunity, Nat. Immunology) and cancer-specific journals (such as Cancer Res. and Oncogene) are used much more frequently comparing to the other two databases. The two other databases are rather oriented towards more generic molecular biology journals as JBC, MCB, Nature and PNAS (Supplemental Figure 3 C, D). We further compared the features of innate immune response representation in different pathway databases. Our innate immune response in cancer resource is the one that contains cell type-specific maps in opposite to other databases. The comparison indicates that the cross talk between the pathways is virtuously represented at the maps of immune response in cancer resource. Finally, the combination of hierarchical organization of knowledge and possibility of navigation through the layers of the maps due to semantic zooming feature makes the innate immune resource more suitable for meaningful data visualisation (Table 3). The visualisation tool box is build-in into the NaviCell environment that allows easy data integration and visualisation in the context of the innate immune maps. Taking together, the results of databases comparison indicate that the innate immune response in cancer resource is topic-specific, that describes immune-related and cancer-relevant signalling processes based on the latest publications about innate immune component in TME. The thoughtful layout and visual organisation of the biological knowledge on the maps makes it a distinguished resource for data analysis and interpretation.

Application of innate immune maps for high-throughput cancer data visualization and analysis

The cell type-specific maps and the meta-map were applied to explore the heterogeneity of innate immune cell types in cancer. The single-cell RNA-Seq data for macrophages and natural killer (NK) cells from metastatic melanoma samples were used (Tirosh et al., 2016).

Polarization and heterogeneity of macrophages population in melanoma

With the help of unsupervised independent component analysis (ICA)-based methodology of gene expression analysis (Hyvärinen and Oja, 2000), we decomposed single cell transcriptome data of Macrophage cells into independent factors. When the single cell RNASeq profiles of individual macrophages were projected in a two-dimensional space (Principal Component 1 and 2), one can see that the independent component computed are attracted by the bimodality

characterizing the distribution (Figure 4A). In order to functionally characterize the biological factor driving this bimodality, data points from the extreme opposite sides of the independent component direction were selected, defining Groups 1 and 2 respectively (see STAR Methods). Then we analyzed potential pro- and anti-tumor properties of these Macrophage cell groups in the context of the innate immunity meta-map. Group 1 has significantly higher anti-tumor score (t-test p-value: 0.02) and Group 2 is the pro-tumor one (t-test p-value: 0.003).

The expression profile differences of the cells from the two groups were interpreted in the context of the Macrophage cell type-specific map and the innate immune response meta-map. The results of the enrichment study for the two Macrophage groups were also represented as heatmaps with a significance level of the p-value for student t-test (see STAR Methods) (Supplemental Figure 4). The module activity values were plotted on the maps using BiNoM plugin of Cytoscape (Bonnet et al., 2013).

Visualization of the data in the context of macrophage cell type-specific demonstrates that the module ‘Antigen presentation’ is upregulated in Macrophage Group 1 (Figure 4B) comparing to Macrophage Group 2 (Figure 4C). Whereas, Macrophage Group 2 (Figure 4C) shows upregulated modules ‘Core signalling pathways’ and ‘Immunosuppressive cytokines pathways’ comparing to Macrophage Group 1 (Figure 4B).

Then, the expression data for the two Macrophage cell groups were analysed in the context of the meta-map that allowed to detect several additional modules differentially regulated between the two groups. The four modules ‘Antigen presentation’ ‘Immunosuppressive checkpoints’, ‘Danger signal modules’ and ‘Immunostimulatory MiRNA and TF’ were significantly overexpressed in Anti-tumor Macrophage Group 1 (t-test p-values respectively: $<10^{-4}$, 0.009, $<10^{-8}$, $<10^{-5}$, Figure 4C) comparing to Pro-tumor Macrophage Group 2 (Figure 4D and E). In contrary, the three modules ‘Recruitment of immune cells module’, ‘Tumor Growth’ and ‘Immunosuppressive cytokine expression’ were strongly upregulated in Pro-tumor Macrophage Group 2 (t-test p-values respectively: $<10^{-6}$, $<10^{-6}$, $<10^{-5}$, Figure 5D). in comparison to Anti-tumor Macrophage Group 1 (Figure 4 D and E).

From these results, it can be concluded that the Macrophage Group 1 has a tendency to express an *anti-tumor phenotype*, because it is characterized by expression of inflammatory cytokines that are able to induce local adaptive immunity via Antigen presentation process. Interestingly, the most typical modules responsible for tumor elimination as ‘Exocytosis and Phagocytosis’ and ‘Immunostimulatory cytokine pathways’ are not over-activated in this cell subset.

In contrary, Macrophage Group 2 demonstrate a *pro-tumor phenotype*, characterized by expression of both, immunosuppressive cytokines restricting local immune response and growth factors supporting tumor growth.

Polarization and heterogeneity of natural killer cells population in melanoma

After using as previously ICA decomposition to group samples, we computed the module activity scores of each group and then a t-test to evaluate the difference in module activity between two NK subpopulations (Group 1 referred to as “tumor-killing” and Group 2 referred to as “immunosuppressed”). (Figure 5A, Supplemental Figure 5A and Supplemental Figure 5B).

First, the comparison and visualisation of the module activity between the two NK cells groups demonstrated activation

of ‘Lytic granules exocytosis’ module in NK Group 1 (the ‘tumor-killing group’) (Figure 5B) comparing to NK Group 2 (the ‘immunosuppressed group’) (Figure 4B) (t-test p-value: 0.006), on the NK cell type-specific map. The activity of this module is directly responsible for tumor killing capacity of NK Group 1 cells that most probably exposes stronger anti-tumor abilities comparing to Group 2. Next, the two NK cells groups were analysed in the context of the meta-map that allowed to detect five differentially regulated modules between the two groups of NK cells. The four modules ‘Recruitment of immune cells’, ‘Integrins’, ‘Fc receptors’, ‘Danger signal pathway’ were significantly upregulated in the NK Group 1 comparing to the NK Group 2 (t-test p-values respectively: 0.0001, $<10^{-4}$, 0.004, $<10^{-5}$). In contrary, the module ‘Immunosuppressive MiRNA and TF’ was inhibited in the NK Group 1 comparing to the NK Group 2 (t-test p-value: 0.001). Finally, although the activity of ‘Phagocytosis and Exocytosis’ module is not significantly different between the two groups, this module is rather activated in the NK Group 1 comparing to the NK Group 2.

Collectively these results demonstrate that the NK Group 1 is characterised by upregulation of biological functions related to NK cell recruitment and activation, coinciding with upregulation of the mechanisms responsible for tumor killing. Thus, the NK Group 1 can be interpreted as newly-recruited, actively migrating NKs with strong anti-tumor polarization. In contrary, most probably, NK Group 2 contains resting or suppressed NK cells that do not expose a well-defined phenotype.

Then we decided to explore possible molecular mechanisms that would explain simultaneous activation of upstream map zones (modules ‘Recruitment of immune cells’, ‘Integrins’, ‘Fc receptors’, ‘Danger signal pathway’) and downstream effector modules ‘Phagocytosis and Exocytosis’ at the level of signalling pathways in NK Group 1. We have compared activation of 30 well annotated pathways on the meta-map (each containing more than 10 proteins) between “tumor-killing group” (Group 1) and “immunosuppressed group” (Group 2) and presented results as a heat map (Figure 5C). There are 7 differentially regulated pathways, 5 upregulated in Group 1 (LFA1, CR3, STING, 2B4, FcGR2) and 2 upregulated in Group 2 (IL13, IL18) (t-test p-values <0.05). Within pathways activated in the “tumor-killing group” (Group 1) there are three (LFA1, CR3 and Fc γ RII). The key players of the pathways are presented schematically in Figure 5D. It can be concluded that the meta-map described difference between NK subtypes both on the level of functional modules and signalling pathways.

Innate immune response meta-map as a source of patient survival signatures

To study whether the innate immune response meta-map can be used for assessment of processes contributing to patient survival, we used the list of genes which have correlation with prognosis of patient survival from (Gentles et al., 2015) (see STAR Methods). We first verified the presence of the genes correlating with patient survival from the above study on the innate immune response meta-map. We detected that out of 627 proteins and protein coding genes depicted on the meta-map, 295 are significantly (z-score p-value <0.05) correlated with the patient survival, that represents 47% of the map content (vs. 27% in whole genome study). The genes enriched in the meta-map can be divided into two groups, positively and negatively correlated with the patient survival, which confirms the observation that innate immune system can play a dual role in cancer disease. Interestingly that from the whole genome analysis in the original study by Gentles et al., 2015, it emerges that there is quasi equal proportion of positively and negatively-correlating genes. However, in the innate immune response meta-map, there is a strong predominance of genes with positive

influence on patient survival (Table 2).

In order to highlight biological functions on the innate immune response map associated to positive or negative patient survival, mean values of gene z-scores per meta-modules were calculated and visualized in the context of the innate immunity meta-map (see STAR Methods). As a general trend, the layers ‘Inducers’ and ‘Core signalling’ on the meta-map are more significantly correlated with patient survival, comparing to the layer ‘Effectors’. Further, the modules with biological functions related to anti-tumor activity as ‘Immune response stimulation’ and ‘Tumor recognition’, ‘Recruitment of immune cells’, etc. are positively correlated with patient survival. Interestingly that the module ‘Tumor killing’ is also positive correlated with the patient survival, though not reaching the statistical significance (Table 2 and Supplemental Figure 6). The minority of functional modules related to pro-tumor activity as ‘Tumor growth’, ‘Immunosuppressive core pathways’, ‘Immunosuppressive MiRNA and TF’ are negatively correlating with patient survival (Table 2 and Supplemental Figure 6). Described analysis demonstrates that the meta-map can serve for evaluation of innate immune response signatures associated with patient survival in cancer.

DISCUSSION

The tumor microenvironment (TME) is now recognized as a critical determinant of tumor development and response to therapy. Its study and pharmacological manipulation are hampered by its complexity and plasticity of cellular components. Systems biology approaches are well suited to address either or both of these difficulties. Therefore, systematization and formalization of molecular mechanisms regulating TME in general, and the innate immune component of the system in particular, are needed. This should include the dissection of multiple intracellular interactions, as well as crosstalks between different TME cell populations with tumor cells.

One of the challenges of cancer biology today is understanding the phenomena of tumor heterogeneity. It consists of two relatively independent parts. First, it is a heterogeneity of the tumor cells themselves, as a result of their clonal divergence or action of epigenetic mechanisms. Second, it is a natural heterogeneity of tumor microenvironment (TME). The last years’ discoveries have shown that understanding how the components of this multi-cellular TME system interact with each other is very important for effective drug design. Actually, the attempt for modulation of the interactions in the tumor microenvironment lies in the basis of new anti-cancer immune check-point therapy.

One of the obstacles hindering the progress in the field is a large number of disconnected experimental data that are not integrated to create a holistic picture. In order to gather together the dispersed scientific knowledge, we have built the set of comprehensive network maps of innate immune response in cancer.

Analysis of large amount of scientific information and search for optimal forms of its representation required development of new approaches for network map construction and annotation. Our first goal was to preserve the natural multidimensionality of the biological knowledge available for different cell type in the innate component of TME. Indeed, different cells types in innate immune system are studied from different angles. Some signalling pathways are described in detail for the macrophages and others for natural killer cells and so on. It is clear that the molecular knowledge described for one cell type cannot be always extrapolated to another. This motivated us to create two complementary representations of innate immune system in cancer, one in the form of cell type-specific maps and the

second, as an integrated meta-map of innate immune response in cancer. To be able to trace the correspondence of molecular entities and processes to a particular cell type, we introduced a system of cell type-specific tags, included in to the annotation of all entities on the maps.

Our second goal was to provide a complete, but not too controversial picture on the processes occurring in the TME. Generation of an integrated meta-map of innate immunity immediately exposed a problem of map complexity. We coped with the complexity problem by introducing the hierarchical structure into the integrated meta-map, respecting the biological functions. The general layout of the integrated meta-map is based on the idea of immune cells polarization in TME, reflected in the representation of both, pro-tumor and anti-tumor signalling mechanisms leading to the corresponding phenotypes and the signalling responsible for a switch in the polarization state. In accordance with the literature, all functional modules and meta-modules on the map are grouped into the pro-tumor and anti-tumor zones.

The modular hierarchical map structure and complex tagging system of maps entities facilitated generation of geographical-like easily browsable open source repository. Taking an advantage of NaviCell platform, that provides Google Maps-engine and map navigation features, the innate immune maps can be explored in an intuitive way, allowing shuttling between the cell type-specific map to the integrated meta-map.

NaviCell-based representation of the maps facilitates visualization of various types of omics data. Analysis of data in the context of both, cell type-specific and integrated maps can help in the formalization of biological hypotheses for the processes and interactions that are studied in some cell types, but unexplored in others. In addition, thanks to the rich system of tags, the maps content can be used as a source of knowledge-based gene signatures of innate immune cell type. Finally, hierarchical organization of the map provides a basis for structural network analysis, complexity reduction and eventual transformation of the map into executable mathematical models.

The resource of innate immune maps is useful for computing network-based molecular signatures of innate immune cells polarization. These signatures will help to characterize the overall status of the signalling dictating pro-tumor and anti-tumor states of TME in cell lines and tumoral samples. It will also help to stratify cancer patients according to the status of the TME and potentially predict patient survival and response to immunotherapies. In addition, the resource might potentially provide new immunotherapy targets, among innate immunity components of TME in tumor infiltrates. These targets can be complementary or synergistic to the well-known immune checkpoint inhibitors.

Construction of innate immune response map is the first step in the attempt to build a global network describing molecular interactions in TME. The next perspective is to represent the knowledge on adaptive immune response and non-immune components in the tumor environment, as fibroblasts and endothelial cells. The final goal is to build a complete map of signalling in cancer representing both intracellular interaction of tumor cells and each component in TME and the intra-cellular interactions, describing the coordination between the component of this multicellular system.

ACKNOWLEDGMENTS

We thank D. Rovera for help with network structure analysis, L. Cristobal Monraz Gomez for help with data visualization and Nicolas Sompairac for help with statistical analysis of maps content. This work has been funded by INSERM Plan Cancer N° BIO2014-08 COMET grant under ITMO Cancer BioSys program. This work received support from MASTODON program by CNRS (project APLIGOOGLE) and COLOSYS grant ANR-15-CMED-0001-04, provided by the Agence Nationale de la Recherche under the frame of ERA-CoSysMed-1, the ERA-Net for Systems Medicine in clinical research and medical practice. ITMO cancer (AVIESAN) provided 3-year PhD grant and foundation Bettencourt Schueller and Center for Interdisciplinary Research supported the training of the PhD student.

AUTHOR CONTRIBUTIONS

M.K. constructed signalling networks, performed data visualisation and wrote the paper; U.C. performed data analysis and enrichment calculations and wrote the paper; S.D.A. advised during the project and revised the paper; V.S. advised during the project and critically revised and restructured the paper; E.B. advised during the project and revised the paper; A.Z. supervised the data analysis, advised during the project and revised the paper; I.K. led the project and wrote the paper.

DECLARATION OF INTERESTS

The authors declare no competing interests.

REFERENCES

- Ascierto, M., Giorgi, V. De, Liu, Q., Bedognetti, D., Spivey, T.L., Murtas, D., Uccellini, L., Ayotte, B.D., Stroncek, D.F., Chouchane, L., et al. (2011). An immunologic portrait of cancer. *J. Transl. Med.* *9*, 146.
- Becht, E., Giraldo, N.A., Dieu-Nosjean, M.-C., Sautès-Fridman, C., and Fridman, W.H. (2016). Cancer immune contexture and immunotherapy. *Curr. Opin. Immunol.* *39*, 7–13.
- Bellora, F., Dondero, A., Corrias, M.V., Casu, B., Regis, S., Caliendo, F., Moretta, A., Cazzola, M., Elena, C., Vinti, L., et al. (2017). Imatinib and Nilotinib Off-Target Effects on Human NK Cells, Monocytes, and M2 Macrophages. *J. Immunol.* *199*, 1516–1525.
- Bhinder, B., and Elemento, O. (2017). Towards a better cancer precision medicine: Systems biology meets immunotherapy. *Curr. Opin. Syst. Biol.* *2*, 67–73.
- Biswas, S.K., and Mantovani, A. (2010). Macrophage plasticity and interaction with lymphocyte subsets: cancer as a paradigm. *Nat. Immunol.* *11*, 889–896.
- Bonelli, S., Geeraerts, X., Bolli, E., Keirsse, J., Kiss, M., Pombo Antunes, A.R., Van Damme, H., De Vlaminck, K., Movahedi, K., Laoui, D., et al. (2017). Beyond the M-CSF receptor - novel therapeutic targets in tumor-associated macrophages. *FEBS J.*
- Bonnet, E., Calzone, L., Rovera, D., Stoll, G., Barillot, E., and Zinovyev, A. (2013). BiNoM 2.0, a Cytoscape plugin

- for accessing and analyzing pathways using standard systems biology formats. *BMC Syst. Biol.* *7*.
- Breuer, K., Foroushani, A.K., Laird, M.R., Chen, C., Sribnaia, A., Lo, R., Winsor, G.L., Hancock, R.E.W., Brinkman, F.S.L., and Lynn, D.J. (2013). InnateDB: systems biology of innate immunity and beyond—recent updates and continuing curation. *Nucleic Acids Res.* *41*, D1228–D1233.
- Calì, B., Molon, B., and Viola, A. (2017). Tuning cancer fate: the unremitting role of host immunity. *Open Biol.* *7*, 170006.
- Cavalieri, D., Rivero, D., Beltrame, L., Buschow, S.I., Calura, E., Rizzetto, L., Gessani, S., Gauzzi, M.C., Reith, W., Baur, A., et al. (2010). DC-ATLAS: a systems biology resource to dissect receptor specific signal transduction in dendritic cells. *Immunome Res.* *6*, 10.
- Chávez-Galán L., Olleros, M.L., Vesin, D., and Garcia, I. (2015). Much More than M1 and M2 Macrophages, There are also CD169+ and TCR+ Macrophages. *Front. Immunol.* *6*, 263.
- Clark, D.P. (2017). Biomarkers for immune checkpoint inhibitors: The importance of tumor topography and the challenges to cytopathology. *Cancer Cytopathol.*
- Cooper, M.A., Fehniger, T.A., and Caligiuri, M.A. (2001). The biology of human natural killer-cell subsets. *Trends Immunol.* *22*, 633–640.
- Croft, D., Mundo, A.F., Haw, R., Milacic, M., Weiser, J., Wu, G., Caudy, M., Garapati, P., Gillespie, M., Kamdar, M.R., et al. (2014). The Reactome pathway knowledgebase. *Nucleic Acids Res.* *42*, D472-7.
- Dorel, M., Barillot, E., Zinov'yev, A., and Kuperstein, I. (2015). Network-based approaches for drug response prediction and targeted therapy development in cancer. *Biochem. Biophys. Res. Commun.* *464*, 386–391.
- Fridlender, Z.G., and Albelda, S.M. (2012). Tumor-associated neutrophils: friend or foe? *Carcinogenesis* *33*, 949–955.
- Fridlender, Z.G., Sun, J., Kim, S., Kapoor, V., Cheng, G., Ling, L., Worthen, G.S., and Albelda, S.M. (2009). Polarization of tumor-associated neutrophil phenotype by TGF-beta: “N1” versus “N2” TAN. *Cancer Cell* *16*, 183–194.
- Gabrilovich, D.I., and Nagaraj, S. (2009). Myeloid-derived suppressor cells as regulators of the immune system. *Nat. Rev. Immunol.* *9*, 162–174.
- Garg, A.D., More, S., Rufo, N., Mece, O., Sassano, M.L., Agostinis, P., Zitvogel, L., Kroemer, G., and Galluzzi, L. (2017). Trial watch: Immunogenic cell death induction by anticancer chemotherapeutics. *Oncoimmunology* *6*, e1386829.
- Gebremeskel, S., Lobert, L., Tanner, K., Walker, B., Oliphant, T., Clarke, L.E., Dellaire, G., and Johnston, B. (2017). Natural Killer T-cell Immunotherapy in Combination with Chemotherapy-Induced Immunogenic Cell Death Targets Metastatic Breast Cancer. *Cancer Immunol. Res.* *5*, 1086–1097.
- Gentles, A.J., Newman, A.M., Liu, C.L., Bratman, S. V, Feng, W., Kim, D., Nair, V.S., Xu, Y., Khuong, A., Hoang,

C.D., et al. (2015). The prognostic landscape of genes and infiltrating immune cells across human cancers. *Nat. Med.* *21*, 938–945.

Gordon, J.R., Ma, Y., Churchman, L., Gordon, S.A., and Dawicki, W. (2014). Regulatory dendritic cells for immunotherapy in immunologic diseases. *Front. Immunol.* *5*, 7.

Gorenshteyn, D., Zaslavsky, E., Fribourg, M., Park, C.Y., Wong, A.K., Tadych, A., Hartmann, B.M., Albrecht, R.A., García-Sastre, A., Kleinstein, S.H., et al. (2015). Interactive Big Data Resource to Elucidate Human Immune Pathways and Diseases. *Immunity* *43*, 605–614.

Goswami, K.K., Ghosh, T., Ghosh, S., Sarkar, M., Bose, A., and Baral, R. (2017). Tumor promoting role of anti-tumor macrophages in tumor microenvironment. *Cell. Immunol.* *316*, 1–10.

Himberg, J., and Hyvärinen, A. (2003). ICASSO: Software for investigating the reliability of ICA estimates by clustering and visualization. In *Neural Networks for Signal Processing - Proceedings of the IEEE Workshop*, pp. 259–268.

Hyvärinen, A., and Oja, E. (2000). Independent Component Analysis: Algorithms and Applications. *Neural Networks* *13*, 411–430.

Kanehisa, M., Goto, S., Sato, Y., Furumichi, M., and Tanabe, M. (2012). KEGG for integration and interpretation of large-scale molecular data sets. *Nucleic Acids Res.* *40*, D109-14.

Kitano, H., Funahashi, A., Matsuoka, Y., and Oda, K. (2005). Using process diagrams for the graphical representation of biological networks. *Nat. Biotechnol.* *23*, 961–966.

Kolde, R. (2012). Package ‘pheatmap’. Bioconductor 1–6.

Kondratova, M., Barillot, E., Zinovyev, A., and Kuperstein, I. (2016). Knowledge Formalization and High-Throughput Data Visualization Using Signaling Network Maps. *bioRxiv* 089409.

Kreuzinger, C., Geroldinger, A., Smeets, D., Braicu, E.I., Sehouli, J., Koller, J., Wolf, A., Darb-Esfahani, S., Joehrens, K., Vergote, I., et al. (2017). A Complex Network of Tumor Microenvironment in Human High-Grade Serous Ovarian Cancer. *Clin. Cancer Res.*

Kuperstein, I., Cohen, D.P.A., Pook, S., Viara, E., Calzone, L., Barillot, E., and Zinovyev, A. (2013). NaviCell: a web-based environment for navigation, curation and maintenance of large molecular interaction maps. *BMC Syst. Biol.* *7*, 100.

Kuperstein, I., Bonnet, E., Nguyen, H.-A., Cohen, D., Viara, E., Grieco, L., Fourquet, S., Calzone, L., Russo, C., Kondratova, M., et al. (2015). Atlas of Cancer Signalling Network: a systems biology resource for integrative analysis of cancer data with Google Maps. *Oncogenesis* *4*, e160.

Laoui, D., Van Overmeire, E., Movahedi, K., Van den Bossche, J., Schouppe, E., Mommer, C., Nikolaou, A., Morias, Y., De Baetselier, P., and Van Ginderachter, J.A. (2011). Mononuclear phagocyte heterogeneity in cancer: Different

subsets and activation states reaching out at the tumor site. *Immunobiology* *216*, 1192–1202.

Mantovani, A., Marchesi, F., Malesci, A., Laghi, L., and Allavena, P. (2017). Tumour-associated macrophages as treatment targets in oncology. *Nat. Rev. Clin. Oncol.* *14*, 399–416.

Marichal, T., Tsai, M., and Galli, S.J. (2013). Mast cells: potential positive and negative roles in tumor biology. *Cancer Immunol. Res.* *1*, 269–279.

Martinez, F.O., Gordon, S., Locati, M., and Mantovani, A. (2006). Transcriptional profiling of the human monocyte-to-macrophage differentiation and polarization: new molecules and patterns of gene expression. *J. Immunol.* *177*, 7303–7311.

Marvel, D., and Gabrilovich, D.I. (2015). Myeloid-derived suppressor cells in the tumor microenvironment: expect the unexpected. *J. Clin. Invest.* *125*, 3356–3364.

Mittal, D., Gubin, M.M., Schreiber, R.D., and Smyth, M.J. (2014). New insights into cancer immunoediting and its three component phases--elimination, equilibrium and escape. *Curr. Opin. Immunol.* *27*, 16–25.

Moynihan, K.D., and Irvine, D.J. (2017). Roles for Innate Immunity in Combination Immunotherapies. *Cancer Res.* *77*, 5215–5221.

Murray, P.J., and Wynn, T.A. (2011). Obstacles and opportunities for understanding macrophage polarization. *J. Leukoc. Biol.* *89*, 557–563.

Le Novère, N., Hucka, M., Mi, H., Moodie, S., Schreiber, F., Sorokin, A., Demir, E., Wegner, K., Aladjem, M.I., Wimalaratne, S.M., et al. (2009). The Systems Biology Graphical Notation. *Nat. Biotechnol.* *27*, 735–741.

O’Hara, L., Livigni, A., Theo, T., Boyer, B., Angus, T., Wright, D., Chen, S.-H., Raza, S., Barnett, M.W., Digard, P., et al. (2016). Modelling the Structure and Dynamics of Biological Pathways. *PLoS Biol.* *14*, e1002530.

O’Sullivan, T., Saddawi-Konefka, R., Vermi, W., Koebel, C.M., Arthur, C., White, J.M., Uppaluri, R., Andrews, D.M., Ngiow, S.F., Teng, M.W.L., et al. (2012). Cancer immunoediting by the innate immune system in the absence of adaptive immunity. *J. Exp. Med.* *209*, 1869–1882.

Ostrand-Rosenberg, S., and Sinha, P. (2009). Myeloid-derived suppressor cells: linking inflammation and cancer. *J. Immunol.* *182*, 4499–4506.

Van Overmeire, E., Laoui, D., Keirsse, J., Van Ginderachter, J.A., and Sarukhan, A. (2014). Mechanisms Driving Macrophage Diversity and Specialization in Distinct Tumor Microenvironments and Parallelisms with Other Tissues. *Front. Immunol.* *5*, 127.

Palucka, K., and Banchereau, J. (2012). Cancer immunotherapy via dendritic cells. *Nat. Rev. Cancer* *12*, 265–277.

R Core Team (2013). R: A Language and Environment for Statistical Computing. R Found. Stat. Comput. Vienna, Austria *0*, {ISBN} 3-900051-07-0.

Raza, S., Robertson, K.A., Lacaze, P.A., Page, D., Enright, A.J., Ghazal, P., and Freeman, T.C. (2008). A logic-based diagram of signalling pathways central to macrophage activation. *BMC Syst. Biol.* 2, 36.

Theoharides, T.C., and Conti, P. (2004). Mast cells: the Jekyll and Hyde of tumor growth. *Trends Immunol.* 25, 235–241.

Tirosh, I., Izar, B., Prakadan, S.M., Wadsworth, M.H., Treacy, D., Trombetta, J.J., Rotem, A., Rodman, C., Lian, C., Murphy, G., et al. (2016). Dissecting the multicellular ecosystem of metastatic melanoma by single-cell RNA-seq. *Science* (80-). 352, 189–196.

Tokunaga, R., Zhang, W., Naseem, M., Puccini, A., Berger, M.D., Soni, S., McSkane, M., Baba, H., and Lenz, H.-J. (2018). CXCL9, CXCL10, CXCL11/CXCR3 axis for immune activation – A target for novel cancer therapy. *Cancer Treat. Rev.* 63, 40–47.

Topalian, S.L., Drake, C.G., and Pardoll, D.M. (2015). Immune Checkpoint Blockade: A Common Denominator Approach to Cancer Therapy. *Cancer Cell* 27, 450–461.

Torphy, R., Schulick, R., and Zhu, Y. (2017). Newly Emerging Immune Checkpoints: Promises for Future Cancer Therapy. *Int. J. Mol. Sci.* 18, 2642.

Vesely, M.D., Kershaw, M.H., Schreiber, R.D., and Smyth, M.J. (2011). Natural innate and adaptive immunity to cancer. *Annu. Rev. Immunol.* 29, 235–271.

Vivier, E., Ugolini, S., Blaise, D., Chabannon, C., and Brossay, L. (2012). Targeting natural killer cells and natural killer T cells in cancer. *Nat. Rev. Immunol.* 12, 239–252.

Vo, M.-C., Nguyen-Pham, T.-N., Lee, H.-J., Jaya Lakshmi, T., Yang, S., Jung, S.-H., Kim, H.-J., and Lee, J.-J. (2017). Combination therapy with dendritic cells and lenalidomide is an effective approach to enhance antitumor immunity in a mouse colon cancer model. *Oncotarget* 8, 27252–27262.

Wickham, H. (2009). *ggplot2* Elegant Graphics for Data Analysis.

FIGURE AND TABLE LEGENDS

Figure 1. Map construction workflow and map structure. The scheme demonstrates the steps of meta-map construction starting from collection of cancer specific and innate-immune specific information about individual molecular interactions from scientific publications and databases, manual annotation and curation of this information (steps 1-4), then organisation of this formalized knowledge in form of cell-type specific maps (step 5), and finally integration the cell-type specific networks in one global meta-map of innate immune response in cancer with areas corresponding to biological processes, modules, pro- and anti-tumor polarisation. (step 6)

Figure 2. Cell type-specific maps. Cell type specific networks are visualized at the top-level view, the colourful background indicates boundaries of functional modules of the maps.

Figure 3. Structure of meta-map of innate immune response in cancer. (A). Top view layout of the innate immune meta-map. Functional modules represent key processes involved in pro-tumor and anti-tumor activity of innate immunity in cancer, showed at different zoom levels (0 – polarization and biological processes, 1-functional modules, 2- signalling pathways, molecules, interaction types and annotation details. (B). Signalling pathways in the meta-map structure in a browser window. (C). The network of modules demonstrating cross-talks between biological processes represented on the meta-map. Nodes represent biological processes with the size associated to number of molecules in a process, color of the node is related to pro/anti- tumor polarization (see legend), interactions reflect cross-talk between the biological processes, the thickness of the edge is related to number of interactions and the color to the nature of interactions.

Figure 4. Visualization of modules activity scores demonstrates functional difference between Pro- and Anti-tumor polarized macrophages cells in the context of maps. (A). Macrophages single cells in PC1 and PC2 coordinates space. Two groups, the first and the fourth quartile of distribution along the IC1 axis, are colored distinctly in blue and black. Staining of the Macrophage cell type-specific map with modules activity scores calculated from single cell RNAseq expression data for (B). Macrophages Groups 1 (Anti-tumor) and (C). Macrophages Groups 2 (Pro-tumor) cells. Staining of the innate immune meta-map with modules activity scores calculated from single cell RNAseq expression data for (D). Macrophages Groups 1(Anti-tumor) and (E). Macrophages Groups 2 (Pro-tumor) cells. Color code: Red–upregulated, green- downregulated module activity.

Figure 5. Visualization of modules activity scores using expression data from melanoma natural killers (NK) shows the possible pathways regulated tumor-killing abilities of NK cells in melanoma. NK single cells in PC1 and PC2 coordinates space. Two groups are colored distinctly in blue and black. (A). Map staining of the NK cell type-specific map with modules activity scores calculated from single cell RNAseq expression data for (B). NK Group 1. (C). Heatmap of activity scores in signalling pathways of NK groups. Map staining of the innate immune response meta-map with modules activity scores for (D). NK Group 1 (“tumor killing”) with a zoom into three signalling pathways relating the two upregulated modules: “Danger signal pathways” and “Exocytosis and phagocytosis” with main molecular players named . Color code: Red–upregulated, green- downregulated module activity.

Table 1. Hierarchical modular structure of innate immune response meta-map.

Table 2. Distribution of genes with positive ($z<0$) and negative ($z>0$) correlation with patient survival across functional meta-modules in innate immune response meta-map. Values indicate number of genes.

Table 3. Comparison of innate immune response representation in different pathway databases

STAR METHODS

Maps access and data availability

The cell type-specific maps and meta-map of innate immune response in cancer are freely available for downloading from the NaviCell web page (<http://navicell.curie.fr/pages/maps>) in several exchange formats. The composition of map signaling pathways, modules and meta-modules is provided in a form of GMT files (Supplemental Tables 2 and 3

respectively) suitable for further functional data analysis.

Map and model

Cell type-specific maps and meta-map of innate immune response in cancer were created using the methodology developed in (Kondratova et al., 2016)(Kuperstein et al., 2015). The maps are drawn in CellDesigner diagram editor (Kitano et al., 2005) using Process Description (PD) dialect of Systems Biology Graphical Notation (SBGN) syntax which is based on Systems Biology Markup Language (SBML) (Le Novère et al., 2009). The data model, includes the following molecular objects: proteins, genes, RNAs, antisense RNAs, simple molecules, ions, drugs, phenotypes, complexes. These objects can play role of reactants, products and regulators in a connected reaction network. Edges on the maps represent biochemical reactions or reaction regulations of various types. Different reaction types represent posttranslational modifications, translation, transcription, complex formation or dissociation, transport, degradation and so on. Reaction regulations include catalysis, inhibition, modulation, trigger and physical stimulation. The naming system of the maps is based on HUGO identifiers for genes, proteins, RNAs and antisense RNAs and CAS identifiers for drugs, small molecules and ions.

Manual literature mining

Molecular interactions reported in the scientific articles were manually curated and the information extracted from the papers was used for reconstruction and annotation the maps. Three types of articles were used for map annotation: (i) experimental innate-immunity specific articles directly or indirectly confirming molecular interactions based on mammalian experimental data; (ii) review articles; (iii) experimental articles from non-immune cells that helped to complement the mechanisms present in immune cells (3% of the literature used for the map). In addition, pathways databases were used to retrieve information of the canonical pathways reported for the innate immune signalling general pathway databases (e.g. KEGG, REACTOME, SPIKE SignaLink, EndoNET) or in the immune system-specialized resources such as VirtuallyImmune (<http://www.virtuallyimmune.org>) and InnateDB (www.innatedb.com).

Map tagging system

The annotation of each molecular object on the maps (protein, gene, RNA, small molecule etc) includes several tags indicating participation of the object in: signalling pathways (tag CASCADE:NAME), functional modules (tag MODULE:NAME) and cell type-specific map (tag: MAP:NAME). Each CASCADE obtains the name of the initiating ligand or receptor, in case when several ligands are acting through the same receptor (Supplemental Figure 4). The tags are converted into the links by the NaviCell factory in the process of online map version generation. The links allow to trace participation of entities in different cell type-specific maps and the sub-structure of the same map (pathway, module, biological process) and also facilitate shuttling between these structures.

Map entity annotation

The annotation panel followed the NaviCell annotation format of each entity of the maps includes sections ‘Identifiers’, ‘Maps_Modules’, ‘References’ and ‘Confidence’ as detailed in (Kuperstein et al., 2015). ‘Identifiers’ section provides standard identifiers and links to the corresponding entity descriptions in HGNC, UniProt, Entrez, SBO, GeneCards and

cross-references in REACTOME, KEGG, Wiki Pathways and other databases. ‘Maps_Modules’ section includes tags of modules, meta-modules, and cell type-specific maps in which the entity is implicated (see above). ‘References’ section contains links to related publications. Each entity annotation is represented as a post with extended information on the entity.

Generation of NaviCell map with NaviCell factory

CellDesigner map annotated in the NaviCell format is converted into the NaviCell web-based front-end, which is a set of html pages with integrated JavaScript code that can be launched in a web browser for online use. HUGO identifiers in the annotation form allow using NaviCell tool for visualization of omics data. Detailed guide of using the NaviCell factory embedded in the BiNoM Cytoscape plugin is provided at <https://navicell.curie.fr/doc/NaviCellMapperAdminGuide.pdf>.

High-throughput data source and software

Normalized melanoma dataset from GEO (GSE72056)(Tirosh et al., 2016) were transformed into log expression levels and mean centred. The exploratory analysis and statistical testing was performed and visualized using R packages (ggplot2, stats, pheatmap) (Kolde, 2012; R Core Team, 2013; Wickham, 2009) then MATLAB ICA implementation of FastICA algorithm (Hyvärinen and Oja, 2000) and icasso package (Himberg and Hyvärinen, 2003) to improve the stability. Colored map images were obtained using function “Stain CellDesigner map” from BiNoM Cytoscape plugin (Bonnet et al., 2013) using .xml map files and the mean expression from the analysis described below.

Analytical pipeline

Group definitions

Independent components analysis, which computes numerical vectors of weights that represent independent factors maximizing non-Gaussian signal, was used to sort the data points along the axis of the first independent component (as it was the only stable dimension according to icasso stability analysis). We divided the NK single cells in half depending on the first independent component (IC1) projection score such that Group 1 had positive projection scores and the Group 2 has negative projection scores. As far as Macrophage single cells are concerned, the distribution of the data was remarkably bimodal along the IC1. In order to best interpret the “extreme” tendencies of the cells placed on the opposite side of IC we selected the first and the last quartile of the macrophage scores of IC1 projection. The distinction of the groups plotted in first and the second principal components space (PC1 and PC2) can be seen in Supplemental Figures 4A and 5A.

Activity scores

For groups defined as described above, following procedure was applied for both NK and Macrophages. For each module, 50% of most variant genes were retained without distinction of cells into groups. Subsequently, cells were selected depending on their group attribution and mean of genes were computed per module per group in each map for visualization purposes (map staining and heatmaps).

In order to assess statistically the possible differences between groups, we compared genes retained for each module

between groups of cells with a t-test. The p-values of the t-test were reported on heatmaps with standard code of significance ($*** < 0.001$, $** < 0.01$, $* < 0.05$, $. < 0.1$). The same mean values per group and per module were plotted on the maps.

Enrichment of innate immune response meta-map with patient survival-correlating genes

The data on pan-cancer meta-analysis of expression signatures from ~18,000 human tumors with overall survival outcomes across 39 malignancies were used (Gentles et al., 2015). The 6323 genes with the z-scores (p-value < 0.05) indicating correlation to patient survival were retrieved (Gentles et al., 2015) and overplayed with the gene list from the innate immune response meta-map. Enrichment of the meta-map with the genes significantly positively or negatively-correlated with patient survival were detected using the Chi-square test, using p-value threshold < 0.001 .

SUPPLEMENTAL INFORMATION

Supplemental Figure 1. Entity annotation structure page in NaviCell format.

Supplemental Figure 2. Comparison of InnateDB, REACTOME, KEGG and Innate immune meta-map databases based on gene names content. (A) Visualization of distribution of 188 unique genes from the innate immune response meta-map across map modules. The content of the map was compared with innate immune-related sub-set of pathways from Innate DB, KEGG and REACTOME and 188 unique genes were identified and visualized. (B) Enrichment of functional modules on innate immune response meta-map with the 188 unique genes (percentage) The p-value of the Chi-square-test is reported following the code: $*** < 0.001$, $** < 0.01$, $* < 0.05$.

Supplemental Figure 3. Comparison of InnateDB, REACTOME, KEGG and Innate immune meta-map databases based on publications used for map annotation. (A) Venn diagram showing intersection of the publications annotating the selected pathways (see the main text) from the four different databases. Distribution of (B) publication years and (C) different types of journals annotating the selected pathways (see the main text) from InnateDB, REACTOME and the Meta-map. The peak in the graph indicates papers from 2010-2015 years of publication is indicated by arrow. (D) Relative use of different types of journals for annotation of the selected pathways (see the main text) from InnateDB, REACTOME and the Meta-map databases.

Supplemental Figure 4. Sup-populations study and calculation of modules activity scores using expression data from melanoma macrophage cells. Activity scores of Macrophages in the two groups for (A) cell type-specific map and for (B) meta-map. The p-value of the t-test between gene expression is reported following the code: $*** < 0.001$, $** < 0.01$, $* < 0.05$, $. < 0.1$

Supplemental Figure 5. Sup-populations study and calculation of modules activity scores using expression data from melanoma natural killers (NK) cells. Heatmap of activity scores of each group in modules of (A) cell-type-specific map and (B) meta-map. The p-value of the t-test between gene expression is reported following the code: $*** < 0.001$, $** < 0.01$, $* < 0.05$, $. < 0.1$

Supplemental Figure 6. Meta-map as a potential source of prognostic signatures for patient survival. (A) Visualization of mean z-scores of meta-modules. Blue zones are enriched by genes with a positive correlation to patient survival, yellow zones are enriched by genes correlated with negative patient survival.

Supplemental Table 1. Modular structure of cell type-specific maps.

Supplemental Table 2. List and content of signalling pathways on innate immune meta-map. PROVIDED AS A SEPARATE FILE

Supplemental Table 3. List and content of modules and meta-modules on innate immune meta-map. PROVIDED AS A SEPARATE FILE

Supplemental Table 4. List of pathways and genes content from Innate DB, KEGG and REACTOME used for comparison of innate immune response with these resources. FULL TABLE PROVIDED AS A SEPARATE FILE

Supplemental Table 5. List of unique genes from innate immune response meta-map comparing to gene lists in pathways selected from InnateDB, KEGG and REACTOME for comparison. PROVIDED AS A SEPARATE FILE

Supplemental Table 6. List genes from innate immune response meta-map positively or negatively-correlated with patient survival. PROVIDED AS A SEPARATE FILE

FIGURES & TABLES

1 RETRIEVING CANCER AND INNATE IMMUNE CELLS RELATED PUBLICATIONS



Figure 1

2 CLASSIFYING INFORMATION INTO CELL-SPECIFIC GROUPS



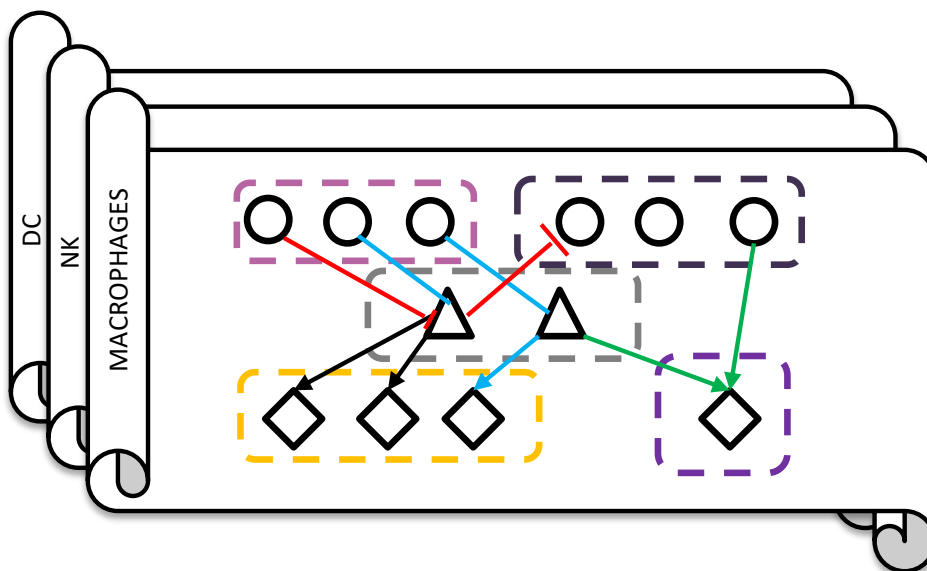
3 MANUAL CURATION OF MOLECULAR INTERACTIONS



4 QUALITY AND REPRODUCIBILITY CHECK



5 KNOWLEDGE ORGANISATION INTO CELL SPECIFIC NETWORK MAPS



ORGANIZATION OF LAYERS

- Molecular type (horizontal)**
- inducers
 - △ intermediates
 - ◇ effectors

- Pathways (up to bottom)**
- activation
 - ↔ inhibition
 - molecular flow

- Functional modules (area)**
- functional module

6 INTEGRATION INTO A META MAP

INHERITS FEATURES OF CELL SPECIFIC MAPS AND IN ADDITION CONTAINS:

- PRO- / ANTI-TUMOR ZONES
- ADDITIONAL NEUTROPHIL AND MAST CELL INTRACELLULAR INTERACTIONS
- CELL-CELL INTERACTIONS
- BIOLOGICAL PROCESSES (GROUPS OF FUNCTIONAL MODULES)

META MAP OF INNATE IMMUNE RESPONSE IN CANCER

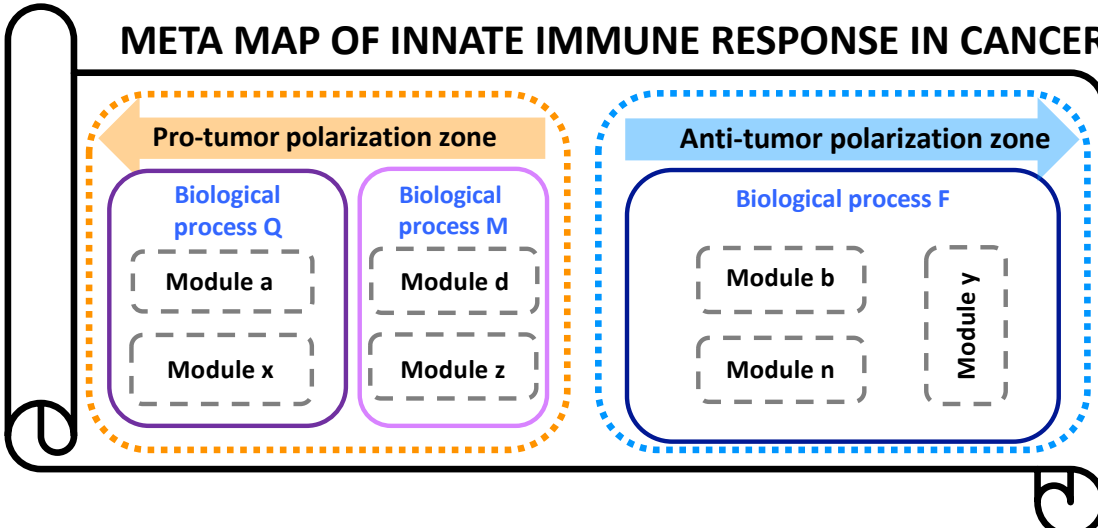


Figure 2

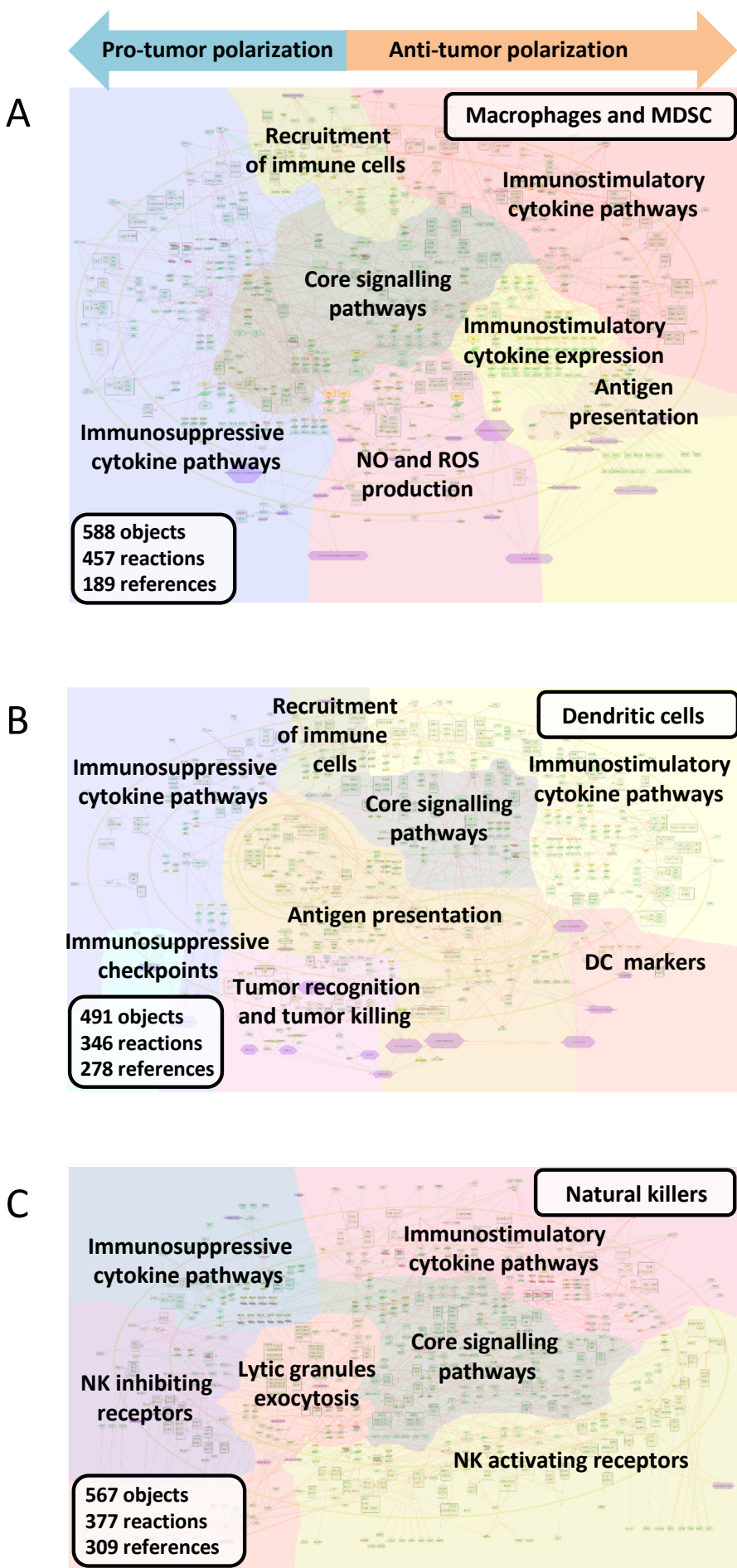
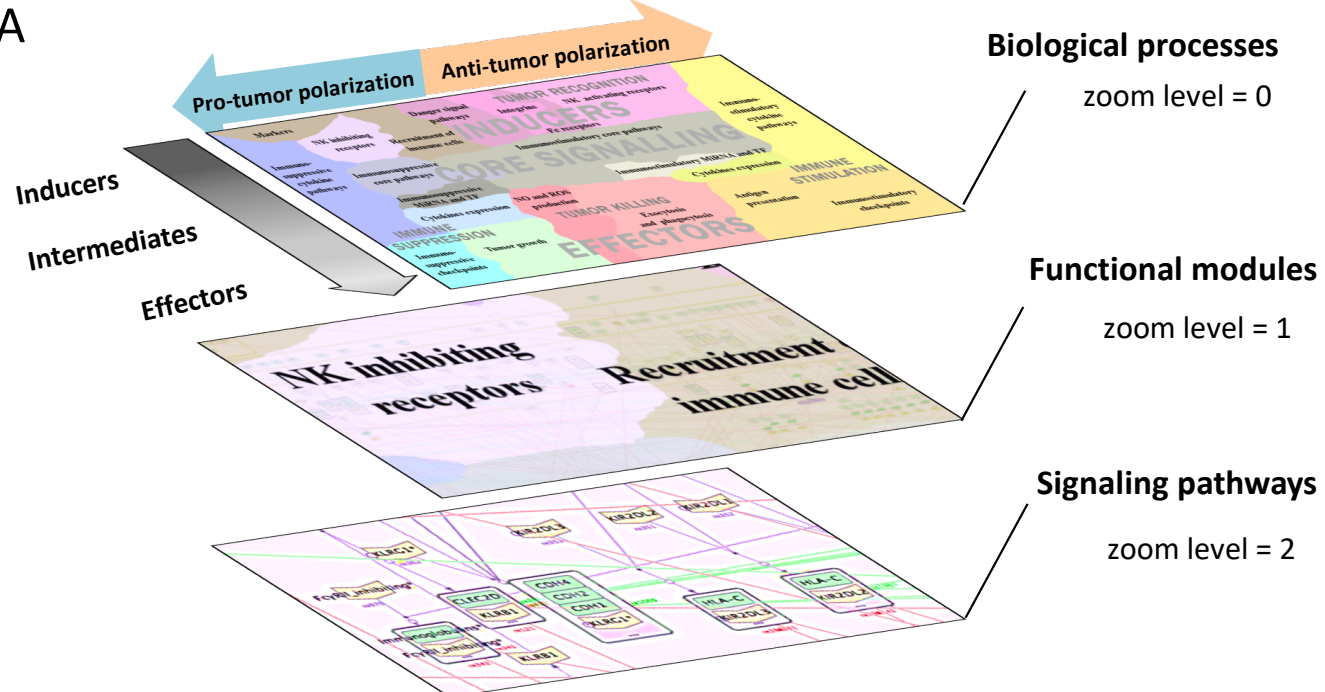


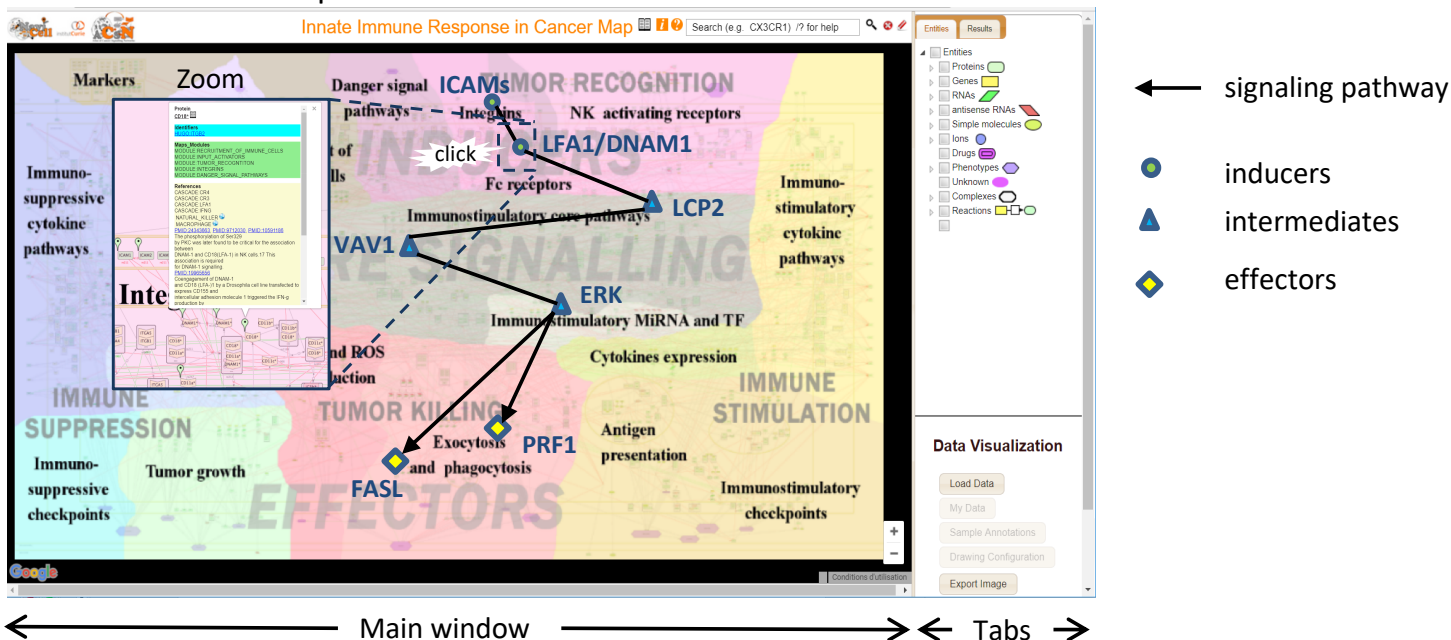
Figure 3

A



B

Screenshot of the map in the browser



C

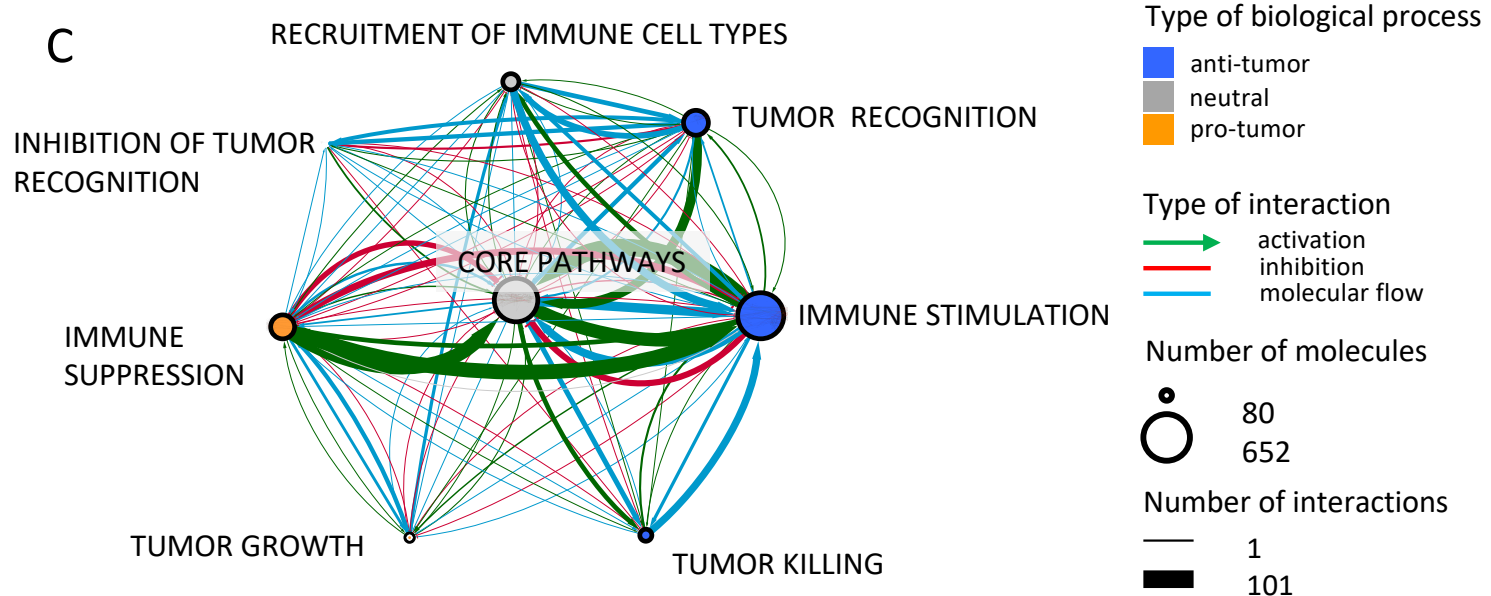
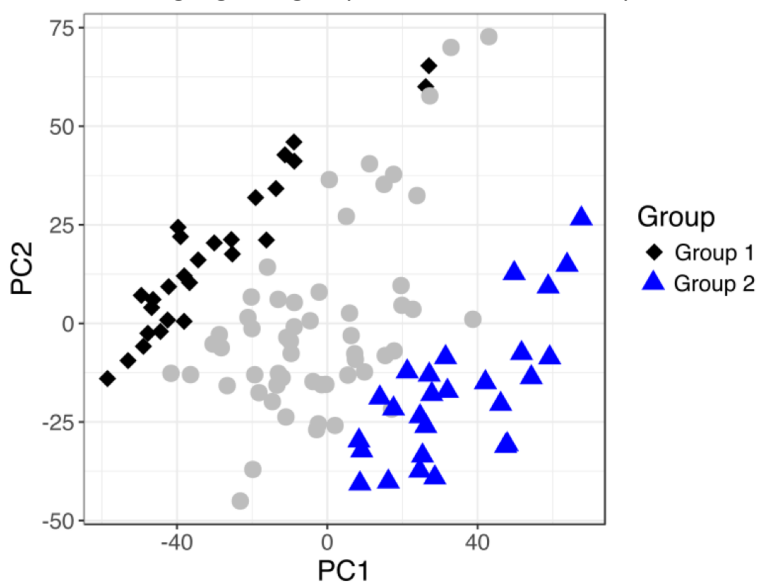


Figure 4

A Macrophages single cells projected in PCA
With highlighted groups based on ICA decomposition



SUMMARY:

Upregulated modules in Anti-tumor Gr 1:

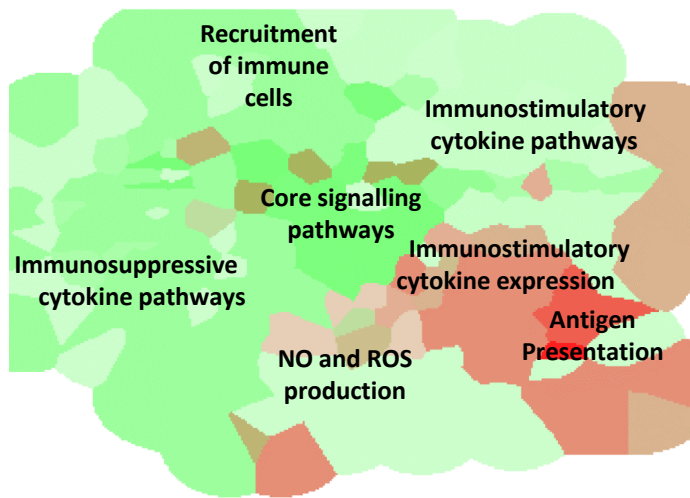
- Antigen presentation (cell-specific and meta map)
- Immunosuppressive checkpoints
- Danger signal modules
- Immunostimulatory MiRNA and TF

Upregulated modules in Pro-tumor Gr 2:

- Tumor Growth
- Immunosuppressive cytokine expression (cell-specific and meta map)
- Recruitment of immune cells module
- Core signalling pathways (cell-specific map)

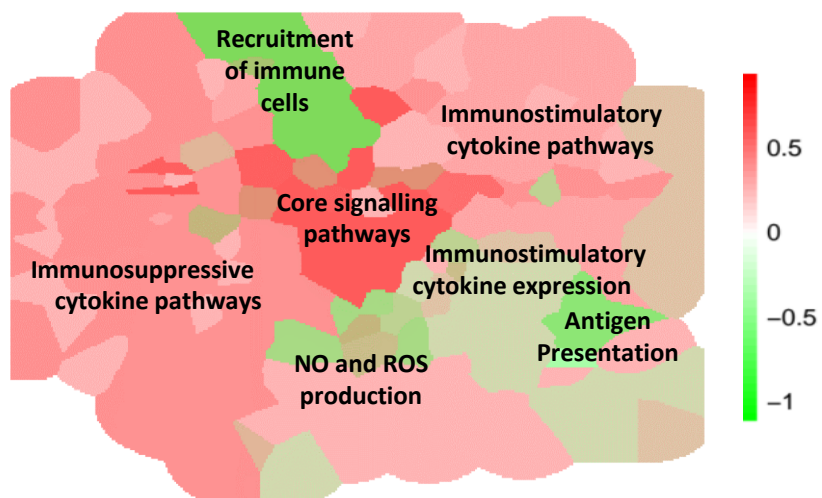
B

Macrophages cell type-specific map: Anti-tumor Group 1



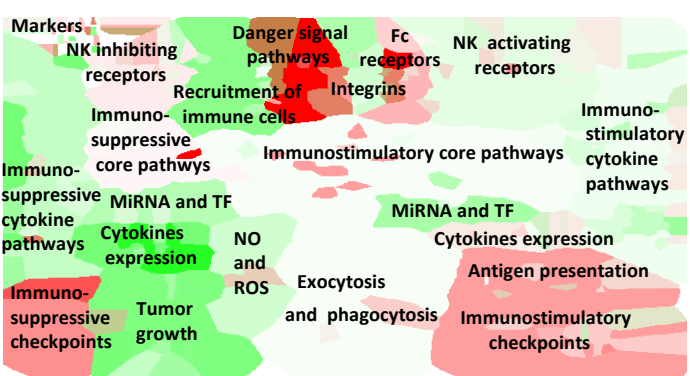
C

Macrophages cell type-specific map: Pro-tumor Group 2



C

Innate immune response meta-map: Anti-tumor Group 1



D

Innate immune response meta-map: Pro-tumor Group 2

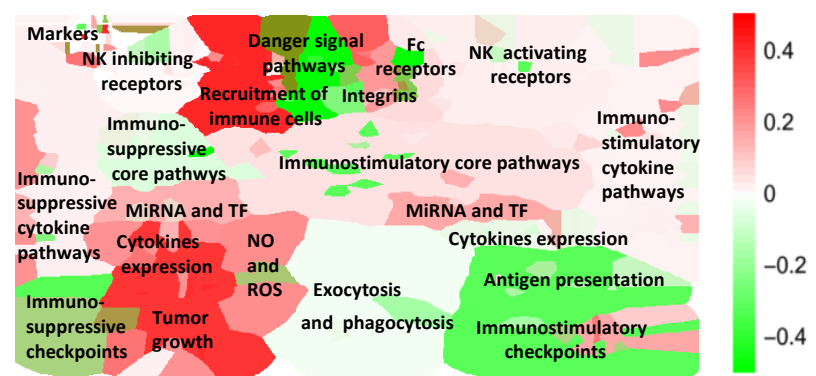
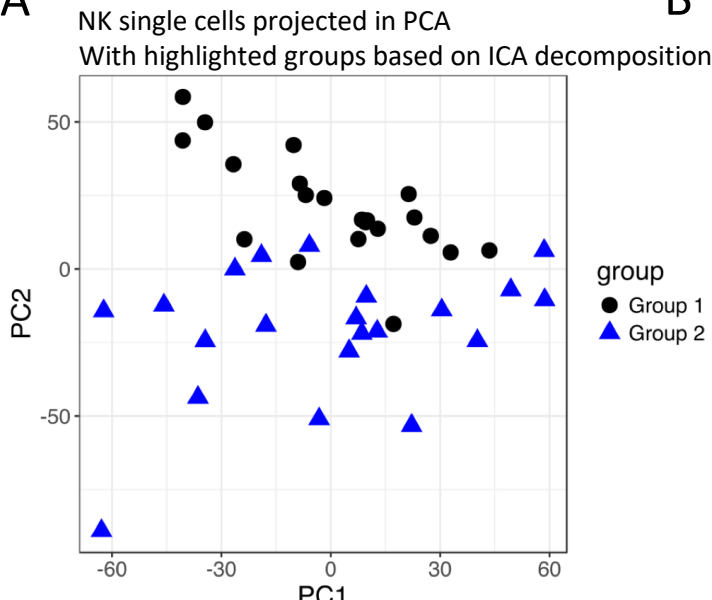


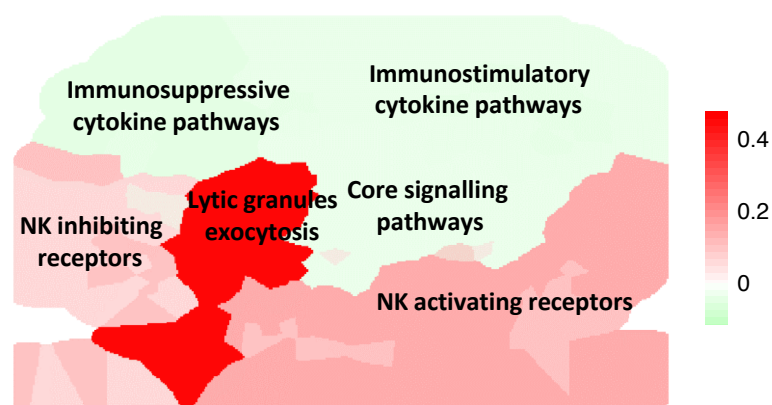
Figure 5

A

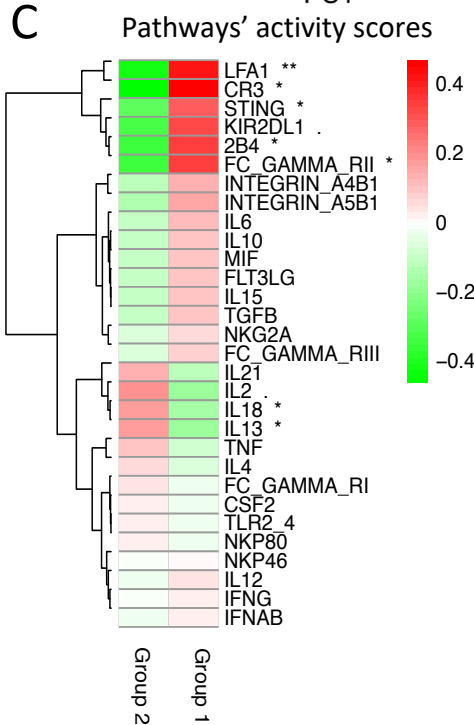


B

NK cell type-specific map: difference Group 1-Group 2

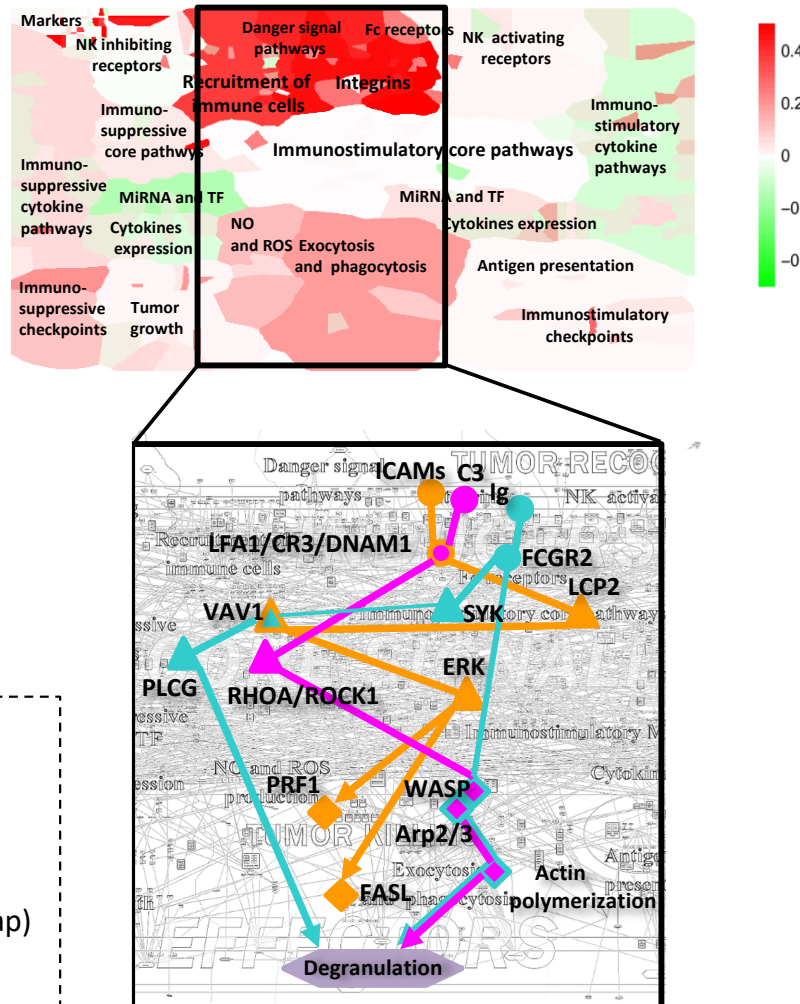


C



D

Innate immune response meta-map: Group 1 (tumor-killing)



SUMMARY:

Upregulated in **Tumor-killing Gr 1**:

- Pathways: LFA1, CR3, STING, 2B4, Fc γ RII
- Modules:
 - Lytic granules exocytosis (cell-specific map)
 - Recruitment of immune cells
 - Integrins
 - Fc receptors
 - Danger signal pathway

Upregulated in **Immuno-suppressive Gr 2**:

- Pathways: IL18, IL13
- Modules:
 - Immunosuppressive MiRNA and TF

Pathways connecting modules 'Integrins' and 'Fc receptors' with 'Phagocytosis and Exocytosis'

- LFA1
- CR3
- Fc γ RII

Table 1: Structure and content of Innate immune meta-map

Zones/Metamodule/Module	Chemical Species (Entities)	Proteins	Genes	RNAs	asRNAs	Reactions	References
Zone: Pro-tumor polarization							
INHIBITION OF TUMOR RECOGNITION							
NK INHIBITING RECEPTORS	35	23	1	1	0	14	57
IMMUNE SUPPRESSION							
IMMUNOSUPPRESSIVE CYTOKINE PATHWAYS	109	46	10	11	3	67	114
IMMUNOSUPPRESSIVE CYTOKINE EXPRESSION	55	19	14	14	0	36	75
IMMUNOSUPPRESSIVE CHECKPOINTS	8	7	0	0	0	8	13
CORE SIGNALLING PATHWAYS							
IMMUNOSUPPRESSIVE CORE PATHWAYS	43	23	5	5	1	25	54
MIRNA TF IMMUNOSUPPRESSIVE	77	20	23	14	12	48	62
TUMOR GROWTH							
TUMOR GROWTH	60	42	8	8	0	71	58
Zone: Anti-tumor polarization							
TUMOR RECOGNITION							
NK ACTIVATING RECEPTORS	114	45	16	14	6	72	115
DANGER SIGNAL PATHWAYS	60	30	2	1	0	36	66
FC RECEPTORS	18	12	0	0	0	8	37
INTEGRINS	38	24	0	0	0	21	56
IMMUNE STIMULATION							
IMMUNOSTIMULATORY CYTOKINE PATHWAYS	152	74	18	18	3	92	193
IMMUNOSTIMULATORY CYTOKINE EXPRESSION	43	17	12	11	1	27	109
ANTIGEN PRESENTATION AND IMMUNOSTIMULATORY CHECKPOINTS	99	65	6	6	0	91	152
CORE SIGNALLING PATHWAYS							
IMMUNOSTIMULATORY CORE PATHWAYS	184	93	6	6	114		244
MIRNA TF IMMUNOSTIMULATORY	50	17	12	10	5	33	60
TUMOR KILLING							
LYtic GRANULES EXOCYTOSIS AND PHAGOCYTOSIS	73	39	6	6	5	50	75
NO ROS PRODUCTION	33	10	4	4	0	23	44
Cell type specific markers							
MARKERS							
MARKERS MACROPHAGE	22	10	6	6	0	0	8
MARKERS NK	10	10	0	0	0	0	36
MARKERS MAST	6	6	0	0	0	0	9
MARKERS DC	16	14	0	2	0	0	14
MARKERS NEUTROPHILE	11	11	0	0	0	0	15
MARKERS MDSC	9	9	0	0	0	0	9
Recruitment							
RECRUITMENT OF IMMUNE CELLS							
RECRUITMENT OF IMMUNE CELLS	103	48	17	17	0	93	83
META-MAP							
	1466	582	162	152	20	1084	820

Table 2. Distribution of genes with positive ($z<0$) and negative ($z>0$) correlation with patient survival across functional meta-modules in innate immune response meta-map. Values indicate number of genes.

Innate immune map meta-module	Mean z-score	Positive correlation with patient survival	Negative correlation with patient survival
TUMOR GROWTH	1.3	12	26
INHIBITION OF TUMOR RECOGNITION	-1.86	18	6
TUMOR RECOGNITION	-1.56	67	28
RECRUITMENT OF IMMUNE CELLS	-0.94	29	14
IMMUNE STIMULATION	-0.53	122	87
TUMOR KILLING	-0.5	25	29
CORE SIGNALLING PATHWAYS	-0.46	114	84
IMMUNE SUPPRESSION	-0.33	39	24

Table 3: Comparison of innate immune response representation in different pathway databases

Feature/Database	KEGG	REACTOME	InnateDB	Innate immune response in cancer resource
Cancer specificity	-	-	-	+
Cell-type specificity	-	+/-	+/-	+
Cross-talks between pathways	+/-	+/-	+/-	+
Hierarchical organization of knowledge	-	+	-	+
Semantic zooming	-	+	-	+
Data visualization	-	+	-	+

Supplementary figures & tables

Figure S1

Protein IRF1

Identifiers

HUGO:IRF1

Maps_Modules

MODULE:MACROPHAGE
MODULE:NK
MODULE:CORE_SIGNALING
MODULE:MIRNA_TF_ACTIVATION
CASCADE:IL2
CASCADE:TNF
CASCADE:IFNAB
CASCADE:IFNG
CASCADE:TLR2_4

References

[PMID:11399519](#)

STAT1, IRF1 and NF- κ B interact with NOS2 promoter and cooperatively activate NOS2 expression in macrophages downstream of IFNG.

[PMID:10820262](#)

Probably IFNG induces SOCS1 expression via IRF1 upregulation downstream of STAT1

[PMID:18345002](#)

TNF induces IRF1 expression both through TNFR1 and TNFR2.

TNF induced IFNB expression through IRF1

[PMID:12417340](#)

IRF-8/ICSBP and IRF-1 cooperatively stimulate mouse IL-12 p40 promoter activity in macrophages.

IRF-1 can be acetylated by p300. p300 is recruited to the IL-12p40 promoter depending on both ICSBP and IRF-1 and acts as coactivator.

[PMID:16597464](#)

IRF-8 and IRF-1 are the target genes in activated macrophages.

The expression levels of CXCL16, H28, IL-17R, LIF, MAP4K4, MMP9, MYC, PCDH7, PML, and SOCS7 were significantly increased in macrophages extracted from WT mice following activation for 4 h with IFNG and LPS. However, no changes in the expression of these genes were observed in cells extracted from IRF-8,

IRF1@INNATE_IMMUNE_META_CELL

Modifications:

In compartment: INNATE_IMMUNE_META_CELL

1. IRF1@INNATE_IMMUNE_META_CELL 
2. IRF1|ace@INNATE_IMMUNE_META_CELL 

Participates in complexes:

Participates in reactions:

As Reactant or Product:

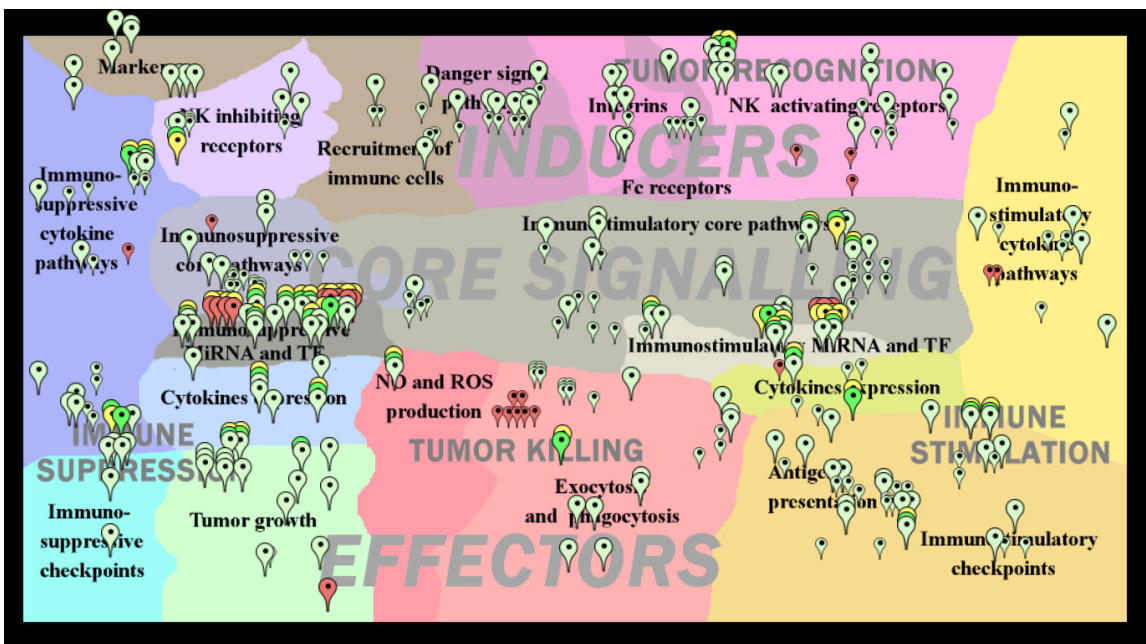
1. [rIRF1@INNATE_IMMUNE_META_CELL](#)  \rightarrow  [rIRF1@INNATE_IMMUNE_META_CELL](#) 
2. [IRF1@INNATE_IMMUNE_META_CELL](#)  \rightarrow  [IRF1|ace@INNATE_IMMUNE_META_CELL](#) 

As Catalyst:

1. [gIDO1@INNATE_IMMUNE_META_CELL](#)  \rightarrow  [rIDO1@INNATE_IMMUNE_META_CELL](#) 
2. [gCXCL16@INNATE_IMMUNE_META_CELL](#)  \rightarrow  [rCXCL16@INNATE_IMMUNE_META_CELL](#) 
3. [gNOS2@INNATE_IMMUNE_META_CELL](#)  \rightarrow  [rNOS2@INNATE_IMMUNE_META_CELL](#) 
4. [gIL12p40*@INNATE_IMMUNE_META_CELL](#)  \rightarrow  [rIL12p40*@INNATE_IMMUNE_META_CELL](#) 
5. [gIFNB*@INNATE_IMMUNE_META_CELL](#)  \rightarrow  [rIFNB*@INNATE_IMMUNE_META_CELL](#) 
6. [gMMP9@INNATE_IMMUNE_META_CELL](#)  \rightarrow  [rMMP9@INNATE_IMMUNE_META_CELL](#) 
7. [gCIITA@INNATE_IMMUNE_META_CELL](#)  \rightarrow  [rCIITA@INNATE_IMMUNE_META_CELL](#) 
8. [gSOCS1@INNATE_IMMUNE_META_CELL](#)  \rightarrow  [rSOCS1@INNATE_IMMUNE_META_CELL](#) 
9. [gMYC@INNATE_IMMUNE_META_CELL](#)  \rightarrow  [rMYC@INNATE_IMMUNE_META_CELL](#) 
10. [gTRAIL*@INNATE_IMMUNE_META_CELL](#)  \rightarrow  [rTRAIL*@INNATE_IMMUNE_META_CELL](#) 

Figure S2

A



B

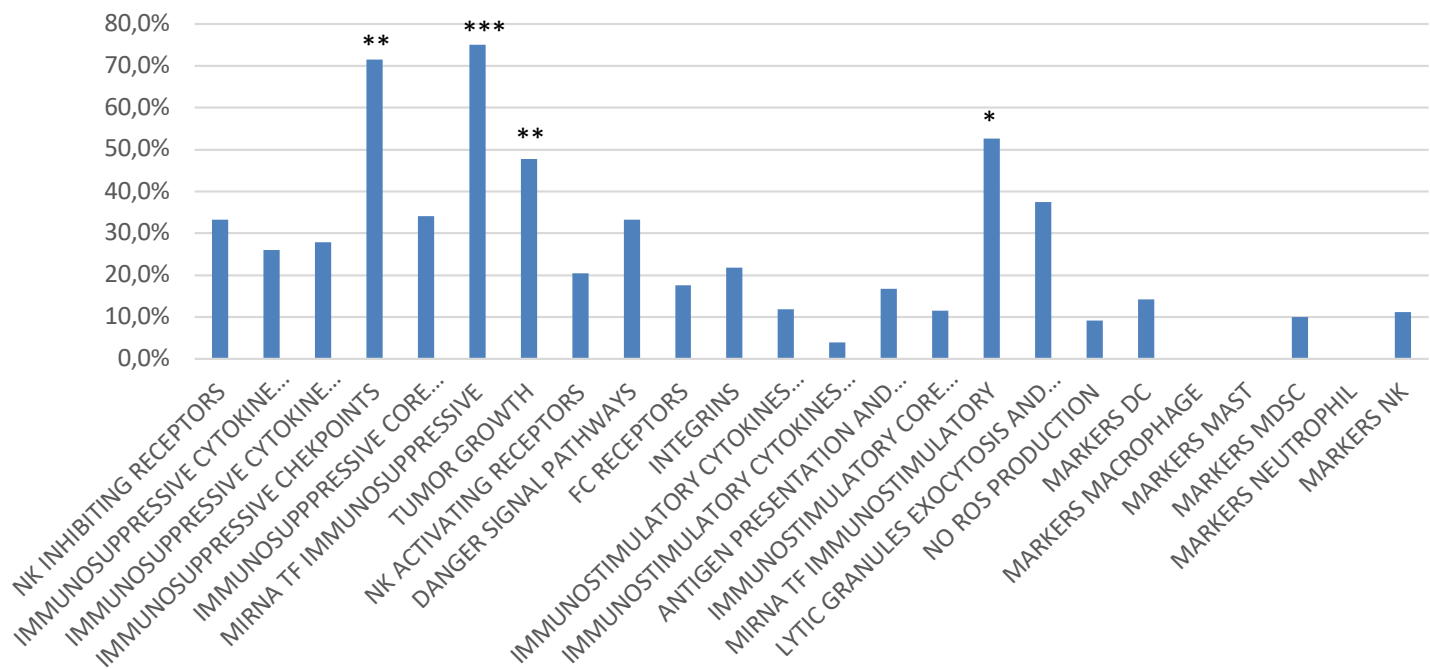
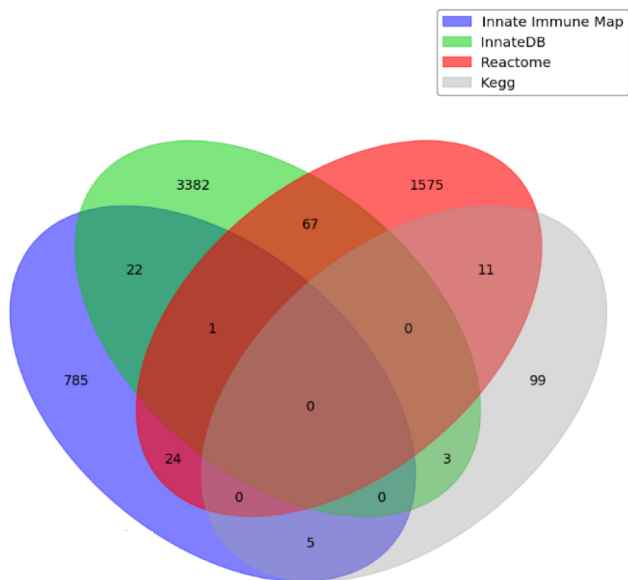
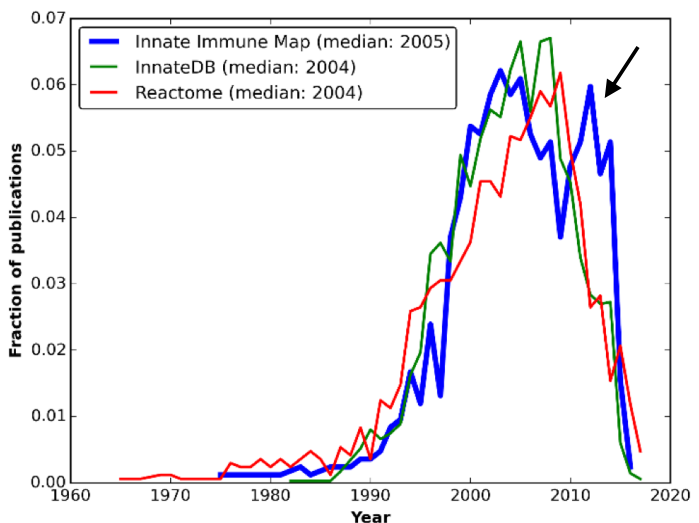


Figure S3

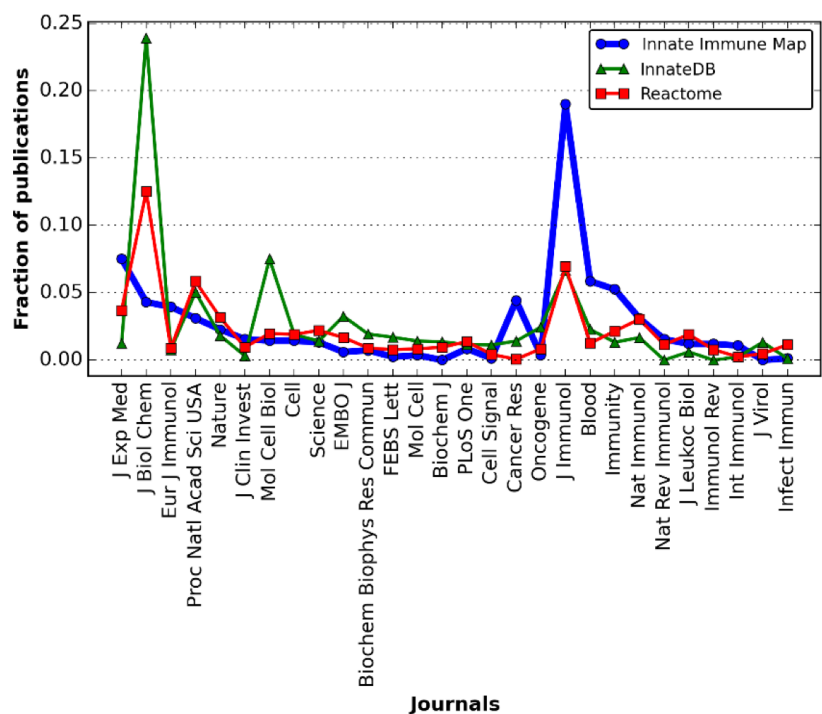
A



B



C



D

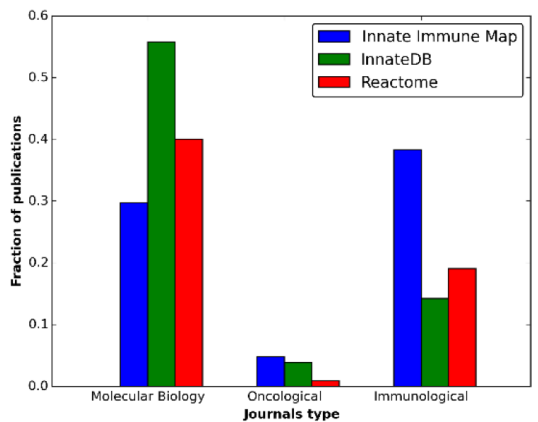


Figure S4

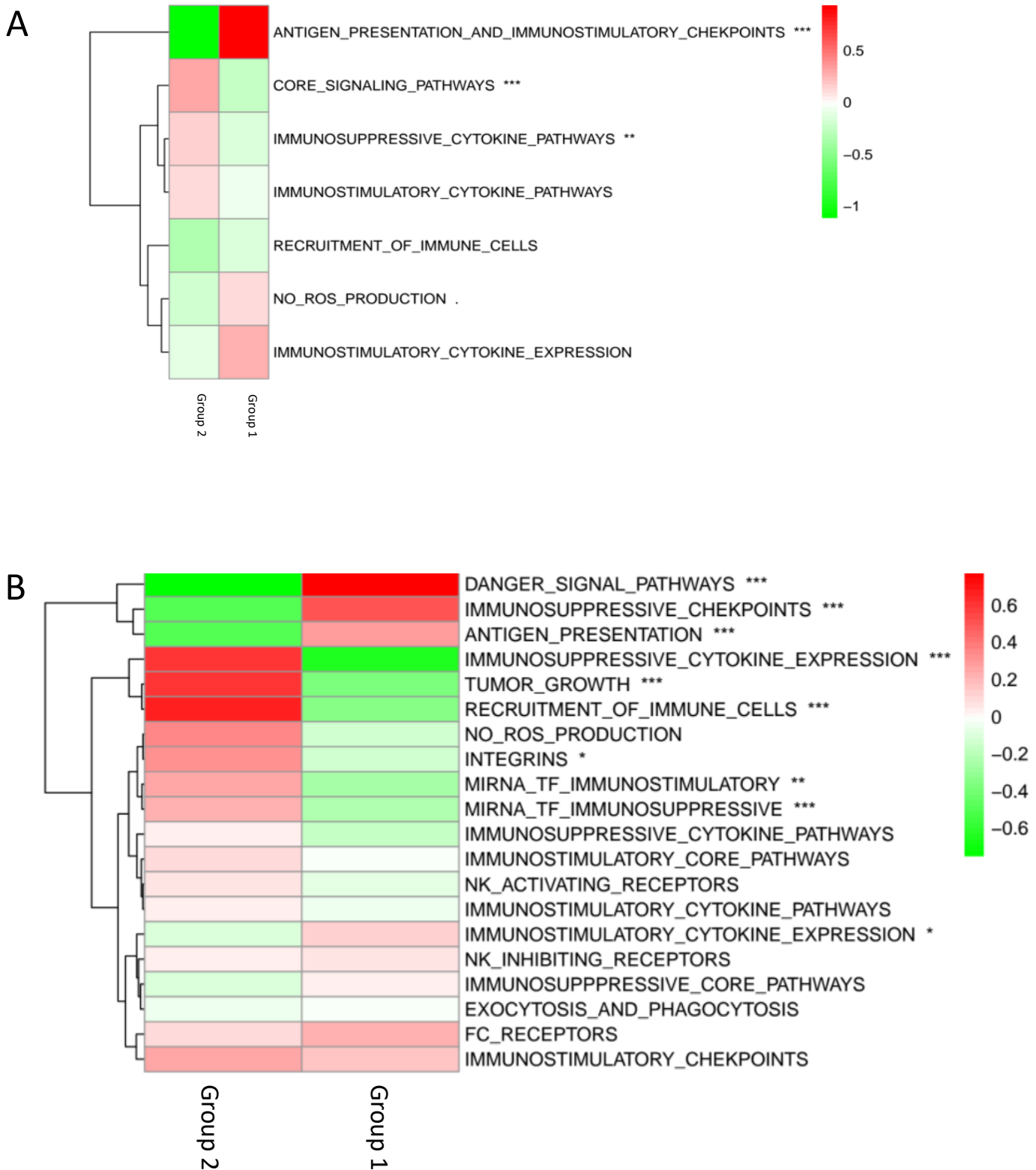


Figure S5

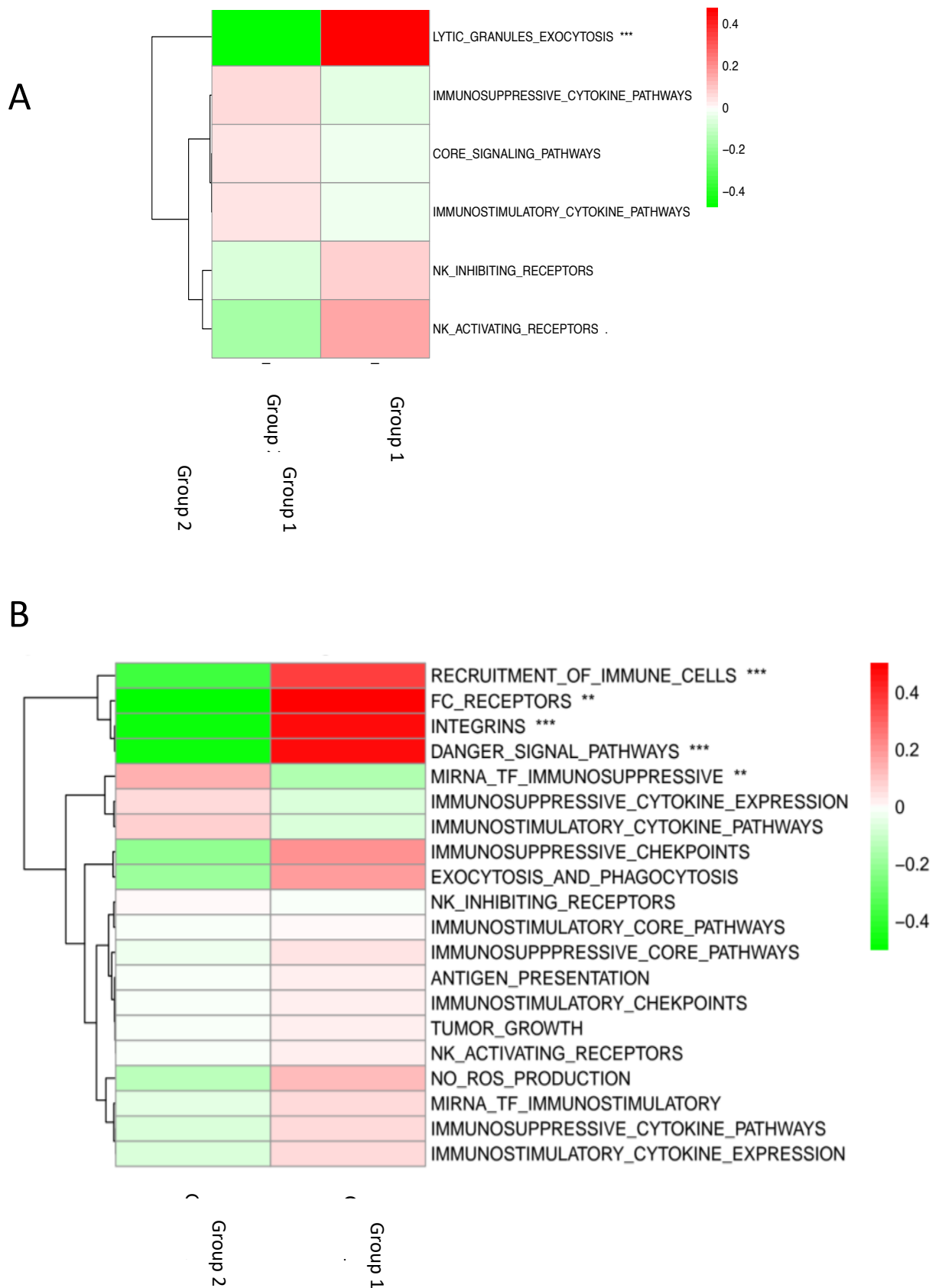
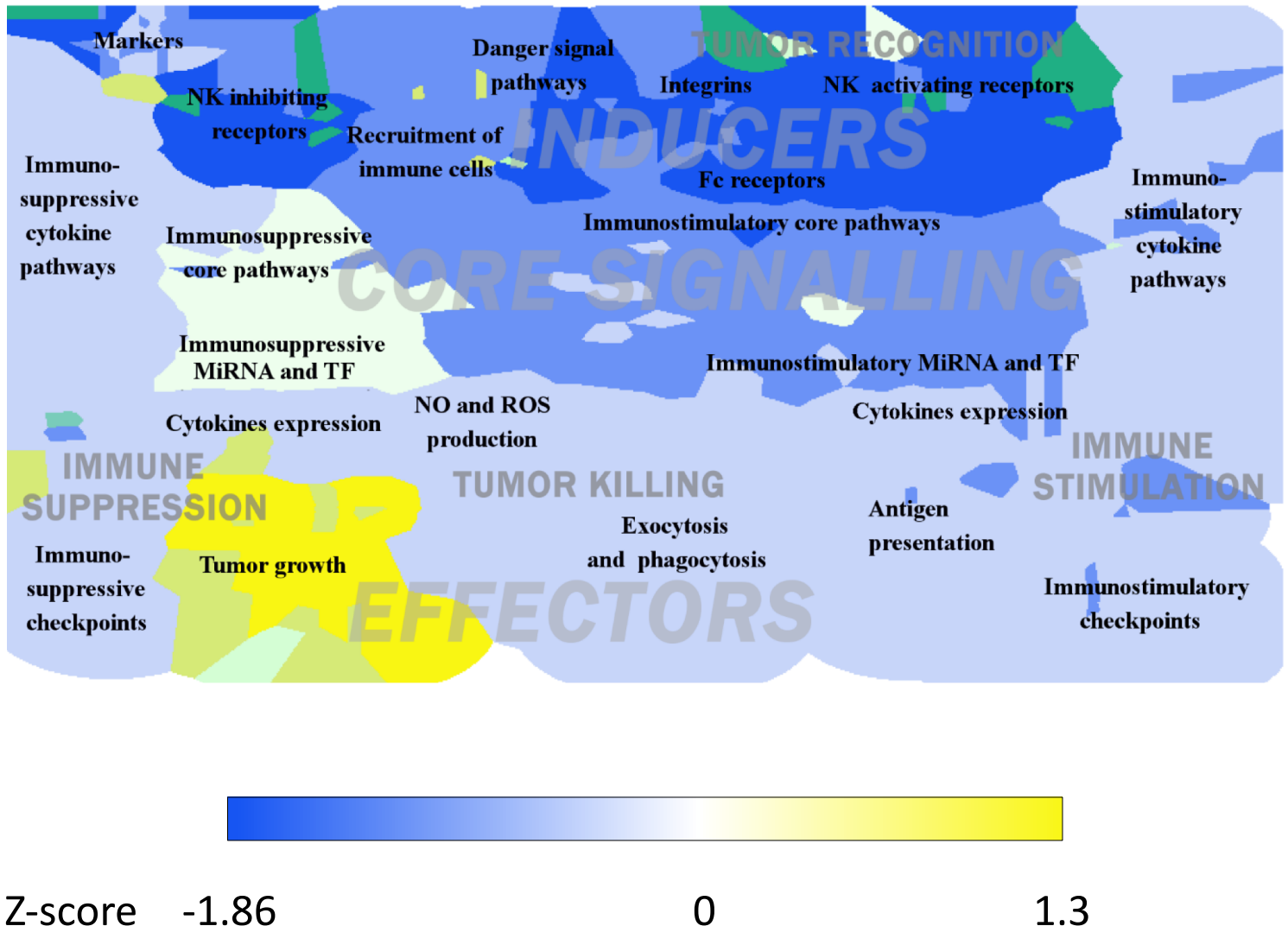


Figure S6



Supplemental Table 1: Structure and content of cell-type specific innate immune maps

Map/Module	Chemical Species	Proteins	Genes	RNAs	asRNAs	Reactions	References
Macrophages and MDSC	588	217	95	95	4	457	189
RECRUITMENT OF IMMUNE CELLS	37	15	6	6	0	29	18
NO ROS PRODUCTION	54	20	6	6	0	37	25
IMMUNOSTIMULATORY CYTOKINE PATHWAYS	92	55	10	9	1	50	75
IMMUNOSTIMULATORY CYTOKINE EXPRESSION	81	31	20	21	0	76	35
ANTIGEN PRESENTATION AND IMMUNOSTIMULATORY CHECKPOINTS	16	5	5	5	0	15	10
CORE SIGNALLING PATHWAYS	144	58	21	21	1	102	58
IMMUNOSUPPRESSIVE CYTOKINE PATHWAYS	163	57	34	33	4	122	82
Natural killers	567	249	53	42	14	377	309
IMMUNOSTIMULATORY CYTOKINES PATHWAYS	107	46	18	15	5	81	89
CORE SIGNALLING PATHWAYS	125	71	5	6	0	140	131
IMMUNOSUPPRESSIVE CYTOKINE PATHWAYS	61	21	14	6	10	38	48
NK INHIBITING RECEPTORS	48	26	2	2	1	31	72
NK ACTIVATING RECEPTORS	124	66	7	8	3	63	142
LYtic GRANULES EXOCYTOSIS	54	34	5	5	5	52	45
Dendritic cells	491	226	43	44	1	346	278
IMMUNOSTIMULATORY CYTOKINES PATHWAYS	132	66	20	21	0	89	125
ANTIGEN PRESENTATION	95	54	5	5	0	81	67
CORE SIGNALLING PATHWAYS	62	33	6	6	1	39	31
IMMUNOSUPPRESSIVE CHECKPOINTS	7	6	0	0	0	6	12
MARKERS DC	10	9	0	0	0	11	12
IMMUNOSUPPRESSIVE CYTOKINE PATHWAYS	58	28	8	8	0	37	52
RECRUITMENT OF IMMUNE CELLS	27	15	4	4	0	23	11
TUMOR RECOGNITION TUMOR KILLING	54	26	2	2	0	37	39

Supplementary Table 4

INNATE DB

Chemokine Signaling Pathway (Human)
Cytosolic DNA-sensing Pathway (Human)
Jak-STAT Signaling Pathway (Human)
MAPK Signaling Pathway (Human)
mTOR Signaling Pathway (Human)
Natural killer cell mediated cytotoxicity (Human)

KEGG -name

	ID
Toll-like receptor signaling pathway	hsa04620
Cytosolic DNA-sensing pathway	hsa04623
Natural killer cell mediated cytotoxicity	hsa04650
Antigen processing and presentation	hsa04612
Fc epsilon RI signaling pathway	hsa04664
Fc gamma R-mediated phagocytosis	hsa04666
Chemokine signaling pathway	hsa04062
Leukocyte transendothelial migration	hsa04670

REACTOME

	ID
Innate Immune System	R-HSA-168249
Interferon Signaling	R-HSA-913531.1
Signaling by Interleukins	R-HSA-449147.7
TNFR2 non-canonical NF-kB pathway	R-HSA-5668541.2
Class I MHC mediated antigen processing & presentation	R-HSA-983169.3
MHC class II antigen presentation	R-HSA-2132295.3